A model for the crystal chemistry of staurolite

M. J. Holdaway, B. L. Dutrow,* Patrick Shore†

Department of Geological Sciences, Southern Methodist University, Dallas, Texas 75275, U.S.A.

Abstract

Previous studies of staurolite have suffered from inadequate knowledge of its chemistry, crystal chemistry, and the relation of these to petrologic occurrence. We provide complete analyses of 31 metapelitic staurolites in an effort to resolve some of these problems. The elements Si, Al, Ti, and Mn show limited variation, whereas H, Fe, Mg, Zn, and Li are highly variable. Analysis of the stoichiometry shows two groups of elements that are each more or less constant in amount: $Si + Al (+ Fe^{3+}?)$, and $R^{2+} + Li + \frac{1}{2}H (+ Ti?)$. The site assignments of Smith are reinterpreted to include dominantly Si and Al in the kyanite layer, Al (and Fe^{3+}?) at the Al(3A) sites, Fe and Mn at the U(1) sites, and Fe, Mg, Zn, Li, (and Ti?) at the ^{iv}Fe sites. Vacant ^{iv}Fe sites are believed to be small in size, whereas the sizes of all the tetrahedral ions at the ^{iv}Fe site are inferred to be 0.025 Å larger than accepted values for tetrahedral sites owing to disorder at the site.

Bond-valence considerations combined with analytical and structural data suggest the following substitutions to be important in staurolite: (1) $^{iv}Si \rightleftharpoons {^{iv}Al}$; (2) $Fe \rightleftharpoons Mg \rightleftharpoons Zn \rightleftharpoons Li$ at the ^{iv}Fe sites; (3) limited substitution involving vacancies at Al(3A), and Mn and Fe at U(1); (4) $2H + \square \rightleftharpoons 2\square + R^{2+}$ involving the P(1A), P(1B), and ^{iv}Fe sites; and (5) possible substitution of Fe^{3+} for Al at the Al(3A) site.

Analysis of staurolites for H_2O and Li_2O is important for calculation of structural formulas. In the absence of such data, microprobe analyses of low-Fe^{3+} staurolites that crystallized with graphite and hematite-free ilmenite should be normalized to $Si + Al = 25.53$. The smaller tetrahedral ions Zn, Li, and Mg and vacancies are expected to become more important in staurolite relative to Fe at elevated P. Natural and synthetic staurolites coexisting with almandine or biotite should have their H and R^{2+} content controlled by P and T such that high-H, low-R^{2+} staurolite is stable at high P and low T; H decreases and R^{2+} increases as T increases and/or P decreases. Staurolites not coexisting with an FeO-saturating phase have higher H, and those coexisting with graphite have lower H.

Introduction

Staurolite is a characteristic mineral of amphibolite-grade pelitic metamorphic rocks. Despite its common occurrence and the many studies that have been done on staurolite, there are still major problems to be resolved regarding its mineralogy and petrology. These problems can be broadly categorized as chemical, crystal chemical, and petrologic.

Chemical problems

Until recently, some aspects of our knowledge of staurolite chemistry were uncertain. Juurinen (1956) provided some of the best analyses in the literature, which included H_2O and Fe^{2+}/Fe^{3+} determinations. Lonker (1983) showed clearly that the H content of staurolite is variable and cannot be associated with a fixed stoichiometry. In a companion paper to the present study, Holdaway et al. (1986) have further characterized the H contents of staurolite and provided ideal values of H-ion contents that permit

the remaining stoichiometry to be calculated. Dutrow et al. (1986), working on the same staurolite specimens, have shown that all of them contain Li, and in one-third, the Li content is more than 0.2 ions per 48-oxygen formula unit. The failure to measure H and Li content of staurolite in the past has led to an incomplete understanding of its chemistry and stoichiometry.

Crystal-chemical problems

Partly because of the lack of complete chemical information and partly because of the chemical complexity of staurolite, crystal-structure determinations have not yielded a full understanding of the crystal chemistry of staurolite. The present knowledge of staurolite crystal chemistry is well summarized by Ribbe (1982). Structure studies of Náray-Szabó and Sasvári (1958), Hanisch (1966) (on a zincian staurolite), Smith (1968), and Tagai and Joswig (1985) have located all the sites, determined approximate levels of site occupancy, and located the atomic positions for most of the Si, Al, Fe, and Zn present in the structure. However, Mg (and recently Li) have posed problems. It has not been possible to locate the Mg with any certainty because its scattering factor is similar to that

* Present address: Institut für Mineralogie, Ruhr-Universität, D-4630 Bochum 1, Federal Republic of Germany.

† Present address: Department of Geology, Stephen F. Austin State University, Nacogdoches, Texas 75961, U.S.A.

of Al. On the basis of chemical studies, Griffen and Ribbe (1973) and Griffen et al. (1982) have proposed possible chemical substitutions, but these authors have assumed constant H content and have not taken into account the possibility of substantial Li in some of their specimens. Ward (1984b) has provided arguments suggesting that the minor Ti present in staurolite occurs at the tetrahedral Fe sites. Takéuchi et al. (1972) have suggested locations for the H ions, recently confirmed by Tagai and Joswig (1985).

The low occupancy of some sites, especially the octahedral Al sites in the iron hydroxide layer (see Fig. 2), and the pseudo-orthorhombic symmetry have led to the suggestion that staurolites may be infinitely twinned (Smith, 1968). Additional evidence of presence of antiphase domains in some staurolites (Fitzpatrick, 1976) led Ribbe (1982) to suggest that Al and vacancies may be partially ordered on the octahedral Al sites of the iron hydroxide layer. Wenk et al. (1974) found evidence for order-disorder in staurolite and observed that the more ordered staurolites formed at high temperatures.

Petrologic problems

There have been serious problems in applying phase-equilibrium studies on the breakdown of staurolite to natural occurrences of the mineral. Reaction of staurolite to kyanite and almandine has been studied experimentally by Ganguly (1972) and by Rao and Johannes (1979). The lower-pressure reaction to sillimanite and almandine has been investigated by Richardson (1968) and recently by Dutrow and Holdaway (in prep.). Application of earlier experimental studies to natural occurrences (e.g., Novak and Holdaway, 1981; Pigage and Greenwood, 1982) has indicated that the experiments predict temperatures substantially higher than those indicated by garnet-biotite geothermometry. The experimental results of Dutrow and Holdaway (in prep.) and the new garnet-biotite geothermometer of Ganguly and Saxena (1984) reduce this discrepancy. The problems of correlation of experimental stability and natural occurrences of staurolite may be explained by several factors. (1) There is no general formula for staurolite that adequately expresses its composition in experiments and in nature. Thus it is difficult to write the experimental reaction correctly. (2) A good activity model that accurately relates natural and experimental compositions is currently unavailable. (3) The entropy of reaction is not well known. Hemingway and Robie (1984) have measured the third-law entropy of staurolite, but the disorder term can only be approximately evaluated. (4) At least one of the experimental studies (Richardson, 1968) indicates temperatures higher than those implied by thermodynamic analyses of the staurolite-kyanite-almandine reaction (Yardley, 1981; Pigage and Greenwood, 1982; Anovitz and Essene, 1982). (5) It is difficult in many pelitic rocks to realistically assess X_{H_2O}, especially in graphite-bearing rocks (Ohmoto and Kerrick, 1977). The first three aspects of this problem, (1) to (3) above, relate directly to inadequate knowledge of the crystal chemistry of staurolite.

This paper reports very careful microprobe analyses of 31 staurolites. When these data are combined with the H_2O analyses of Holdaway et al. (1986) and Li_2O analyses of Dutrow et al. (1986), a set of accurate staurolite stoichiometries is achieved. Using these stoichiometries, we investigate the site occupancies, chemical substitutions, and formulas to arrive at a model for staurolite crystal chemistry that is consistent with available structure determinations and bond-valence considerations. Although this model is consistent with available data, it cannot be considered as the only possible model for staurolite crystal chemistry. The approaches used give general information concerning the site occupancies of most of the ions. Aspects that are still uncertain are (1) whether some Mg resides at more than one site, (2) whether some Al resides at additional sites beyond those discussed, and (3) the site occupancies of the minor elements Mn, Ti, Fe^{3+}, and Li. Careful structure determinations of accurately analyzed staurolites over a wide range of composition will be needed to test and refine the model. In addition, a future project by M.J.H. will involve analysis of some of the present staurolites plus additional specimens for Fe_2O_3 in an effort to cast more light on the location of Fe^{3+}.

EXPERIMENTAL PROCEDURES

Staurolite specimens

The staurolites chosen for study are all from pelitic metamorphic rocks, and all constitute at least 1% of the rock. Thus staurolites from hornblende-bearing rocks (e.g., Spear, 1982) or trace occurrences of Mg-rich staurolites (Ward, 1984a; Schreyer et al., 1984) are excluded. Localities and assemblages are given in Table 1. The specimens in Table 1 are ordered downward on the basis of increasing structural H content. For the four staurolites from Maine collected by M.J.H., a polished section was made of each rock. For all the other staurolites, multispecimen epoxy grain mounts of separated staurolite grains were made for analysis.

Analytical procedure

Microprobe analyses for major and minor elements were done on an automated JEOL-733 microprobe at SMU with KRISEL automation using the correction procedure of Bence and Albee (1968) modified by Albee and Ray (1970). Beam current was 20 nA, accelerating potential 15 kV, and bean diameter 2 μm. Standards included a Mg-bearing garnet for Mg, andalusite for Al, a cordierite for Si, Kakanui kaersutite for Ti, a Mn-rich garnet for Mn, an almandine garnet for Fe, and willemite for Zn. Each major and minor element analysis was for 30 s or 60,000 counts. For the polished sections from Maine, six random analyses from a single staurolite crystal were averaged; for the grain mounts, ten analyses of separate grains were averaged. In no case were any significant compositional variations observed within specimens. After every two specimens were analyzed, four analyses of the andalusite and four of the kaersutite were made. Elements were restandardized after drift of ≥ 1% relative for major elements and ≥ 3% relative for minor elements. Linear drift corrections based on the andalusite and kaersutite analyses were made for Al, Si, Mg, Ti, and Fe.

For trace elements Zr, V, Cr, and Co, a separate analysis scheme (MAGIC, John Colby, Kevex Corp.) was used at 20 kV. Al and Si were fixed at average values, and Mg, Fe, and Zn were included in the analyses. For each staurolite, two grains were analyzed for

Table 1.   Localities and assemblages for staurolite specimens, listed in approximate order of increasing structural H content

Specimen	Locality	Assemblage	References*
3-3	West Sidney, Maine	Bt-Gt-Chl-Crd-And-Ilm	Osberg (1971)
86	Houghton, Maine	Bt-Gt-Chl-Pl-Ilm-Gr	Guidotti (1974)
ER-70	Errol quad, N.H.	Bt-Gt-Ilm	Green (1963)
M-29	Jordan Falls, N.S.	Bt-Gt-Chl-Ilm	Taylor and Schiller (1966)
EH-6	Emery Hill, N.Y.	Bt-Gt-Chl-Ged-Cum-Sil-Crn-Mag	Tracy
164	Houghton, Maine	Bt-Gt-Chl-Sil-Pl-Ilm-Gr	Guidotti (1974)
114-1	Byron, Maine	Bt-Gt-Chl-Ilm-Gr	Holdaway
KF-9	Fernleigh, Ontario	Bt-Ilm-Mag	Hounslow and Moore (1967)
655-1	Ashley Falls quad, Conn.	Bt-Gt-Ky-Pl-Ilm-Mag	Zen (1981)
53-2	East Dixfield, Maine	Bt-Gt-Sil-Ilm-Gr	Holdaway
SL-2	Webusko Lake, Manitoba	Bt-Gt-Ilm	Froese and Gasparrini (1975)
356-1	Bashbish Falls, Conn.	Bt-Gt-Chl-Pl-Ep-Ilm-Mag-Gr	Zen (1981)
SL-1	Snow Lake, Manitoba	Bt-Gt-Ilm	Froese and Gasparrini (1975)
106038	Franklin, N.C.	Gah**	Smithsonian
117183	Fannin Co., Ga.	Bt**	Smithsonian
36764	Windham, Maine	Bt-Gt-Ilm	Smithsonian
CT-DL-1	Glastonbury quad, Conn.	Bt-Gt-Ilm-Gr	London
M-1	Cherokee Co., Ga.	Bt-Gt-Ilm	Griffen
117189	Stratford, N.C.	Gah**	Smithsonian
119551	Mitchell Co., N.C.	Bt-Ilm	Smithsonian
78332	Slatoust, Urals, USSR	Bt-Gt-Ilm-Gr	Smithsonian
6-3	East Winthrop, Maine	Bt-Gt-Sil-Pl-Ilm	Holdaway
B14040	Pizzo Forno, Switzerland	Bt-Pg-Ky	Smithsonian
GTU-104	Anderson Mine, Manitoba	Bt-Chl-Gah	Froese and Gasparrini (1975)
PF-3	Pizzo Forno, Switzerland	Bt-Chl-Ky	Griffen
355-1	Bashbish Falls, Conn.	Gt-Chl-Pl-Ilm-Mag	Zen (1981)
PE-1	Pennsylvania	Bt-Gt-Chl-Ky-Ilm	Griffen
PF-2	Pizzo Forno, Switzerland	Bt-Pg-Chl-Ky	Griffen
77-55c	Truchas Mtns., N.M.	And-IlmHem	Grambling
71-60E	Black Mtn., N.H.	Chl-Cld-IlmHem-Mag	Rumble (1978)
71-62R	Black Mtn., N.H.	Chl-Cld-IlmHem-Mag	Rumble (1978)

Note: All specimens save EH-6 contain quartz and muscovite. Mineral abbreviations (Kretz, 1983): biotite—Bt, paragonite—Pg, garnet—Gt, chlorite—Chl, chloritoid—Cld, cordierite—Crd, gedrite—Ged, cummingtonite—Cum, andalusite—And, sillimanite—Sil, kyanite—Ky, corundum—Crn, plagioclase—Pl, epidote—Ep, gahnite—Gah, ilmenite—Ilm, ilmenohematite—IlmHem, magnetite—Mag, graphite—Gr. Graphite listed only when clearly present.

* Source of specimen provided when reference not available.
** Incomplete assemblage, nearly pure staurolite.

60 s per element. The Ti-V interference was corrected manually. ZrO_2 contents were 0 to 0.08% and are not given in the analyses.

In order to obtain an estimate of the analytical precision, four staurolites were analyzed on two separate days for major and minor elements using the procedure described above. For this particular microprobe and procedure, the relative variance for a given element averaging $\geq 10\%$ was found to be reasonably well predicted by the following empirical expression, a slight modification of standard treatment of counting statistics:

$$\sigma_i^2 = A[N_i^s/(N_i^s)^2 + N_i^u/(N_i^u)^2],$$

where N_i^s is the total number of counts for an element in the standard or the mineral used for normalization, N_i^u is the total number of counts for an element in the unknown, and A is treated as constant (= 2.7) and compensates for short-term electronic and spectrometer drift. For elements present in amounts $\leq 10\%$ on the average, 0.02% of the oxide was added to compensate for background effects. This procedure gives relative 1σ precision of 0.4% for SiO_2 and Al_2O_3, 0.9% for FeO, 1.7% for MgO, 5.8% for ZnO and TiO_2, and 16% for MnO. Using standard error analysis, these percentages were applied to the average stoichiometric amount of each element to give an analytical precision for each (see Table 5). In this procedure, the precision in stoichiometric amount is slightly greater in percentage than the relative error in analysis because of the effect of the other elements on the stoichiometric amount of a given element.

Unit-cell dimensions were determined by D. T. Griffen, Brig-

ham Young University, with a General Electric XRD-5 X-ray powder diffractometer using Ni-filtered $CuK\alpha$ radiation. Scan rate was $2°$ 2θ per minute; beam slit was $1°$, and receiving slit was $0.1°$. A CaF_2 internal standard ($a = 5.4630$ Å) was used, and peaks were indexed following Borg and Smith (1969). Data were refined on the basis of a monoclinic cell using the least-squares refinement program of Evans et al. (1963). To avoid biasing the β angle away from 90°, hkl peaks were indexed as both hkl and $hk\bar{l}$, and $h0l$ peaks as both $h0l$ and $h0\bar{l}$. This procedure produced deviations of β from 90° of no more than 0.001° (see also Griffen and Ribbe, 1973).

Comparison with previous chemical analyses

Whereas the discussion in the previous section addresses the problem of analytical precision, it does not consider analytical accuracy. In a mineral such as staurolite, where neither the stoichiometry nor the total percentage of oxides of elements with atomic numbers greater than or equal to that of F is known, it is extremely difficult to be sure of the accuracy of analyses done with the electron microprobe. In addition, there are imperfections and nonlinearities in all schemes for microprobe-data reduction (e.g., Bence and Holzwarth, 1977) which force the analyst to rely on stoichiometry and totals as a test of accuracy. At the same time, it is imperative that the analyses be as accurate as possible if they are to be used for estimating site populations. With these considerations in mind, we have compared our microprobe analyses with microprobe analyses and wet-chemical analyses by pre-

Table 2. Comparison of analyses of staurolites

	1 (7)	2 (7)	3	4 (2)
SiO_2	-0.30 ± 0.26	0.09 ± 0.29	-0.11	0.20
Al_2O_3	1.02 ± 0.45	-0.17 ± 0.48	0.43	0.73
TiO_2	0.00 ± 0.02	-0.03 ± 0.04	-0.02	0.02
Cr_2O_3	0.03 ± 0.03	n.d.	0.03	n.d.
V_2O_5	-0.01 ± 0.01	n.d.	-0.01	n.d.
CoO	0.01 ± 0.01	n.d.	0.01	n.d.
FeO^t*	-0.54 ± 0.21	-0.59 ± 0.28	-0.57	-0.45
MgO	-0.03 ± 0.11	0.21 ± 0.09	0.09	-0.30
MnO	0.03 ± 0.02	-0.01 ± 0.03	0.01	-0.03
ZnO	-0.10 ± 0.22	0.04 ± 0.15	-0.03	n.d.

Note: Each column represents the average value for an oxide: present results minus previous results in wt%. Columns are as follows: (1) Griffen and Ribbe (1973), who used EMPADR data reduction; (2) Lonker (1983 and unpubl. ms.), who used Bence-Albee; (3) average of the preceding two columns; (4) wet-chemical analyses of Juurinen (1956). In the column headings, ( ) = number of staurolites analyzed in both studies; n.d. = not determined.
* Total Fe as FeO.

vious workers. The sum of all oxides in the present uncorrected analyses is 100.23(30)%,[1] implying that if there are significant errors in accuracy, they must tend to compensate each other.

Table 2 summarizes a direct comparison between the present analyses and 16 analyses of the same staurolites by previous workers. With the exception of the three major oxides SiO_2, Al_2O_3, and FeO^t (=total Fe as FeO), the present analyses seem to agree reasonably well with previous analyses. Although the values for SiO_2 vary somewhat, there seems to be no consistent pattern of variation of the present analyses from previous analyses. However, FeO^t is consistently lower in the present analyses than in all previous analyses. To compensate for this deviation, all the values of FeO^t in the present analyses were multipled by 1.04 to increase the average FeO^t by 0.51, close to the average discrepancy shown in Table 2. As would be expected, there are significant differences between analysts for Al_2O_3. Because of the great difficulty in standardizing for Al_2O_3, more emphasis is placed on the high-quality wet-chemical analyses of Juurinen (1956). The present values are too high and were multiplied by a factor of 0.987, which reduces the average Al_2O_3 content of staurolites previously analyzed by other workers by 0.71. Application of the two correction factors reduces our analytical totals to 100.03(29)%.

The SiO_2 and Al_2O_3 contents of staurolite vary within narrow limits as shown by the present study. Thus a comparison of groups of analyses of these oxides with previous wet-chemical analyses has some merit. Table 3 shows this comparison for several groups of staurolites. There is a pattern of increasing Al_2O_3, decreasing SiO_2, and decreasing standard deviation with average date of analysis which might suggest that quality of analyses improved during the 1940s and 1950s. Comparison of the present corrected results with the wet-chemical analyses suggests that the correction in Al_2O_3 content is warranted. It must be pointed out that group comparisons of this type are only approximate, as different staurolites were analyzed in each study.

The correction in FeO^t is approximately equivalent to using the Kakanui kaersutite for standardization instead of almandine. In no case are the imperfections in the original standardization large enough to have any matrix effect on the amounts of the other elements in the analyses. It is conceivable that our SiO_2 values are slightly low and the Al_2O_3 values are still slightly too

Table 3. Group comparison of wet-chemical analyses with present results for Al_2O_3 and SiO_2

	Al_2O_3*	SiO_2**
Cited by Juurinen, 1956	51.98 ± 1.71 (18)	28.32 ± 1.08 (24)
Deer et al., 1962	52.44 ± 1.39 (8)	27.76 ± 0.75 (8)
Juurinen, 1956	53.04 ± 1.47 (6)	27.67 ± 0.66 (6)
This study (original)	54.69 ± 0.73 (31)	27.39 ± 0.32 (31)
This study (corrected)	53.98 ± 0.72 (31)	27.39 ± 0.32 (31)

Note: Group comparisons—very few of the same staurolites were analyzed. ( ) = number of analyses.
* Excluding an analysis with zero H_2O and six analyses with >3% Fe_2O_3.
** Excluding analysis with zero H_2O.

high (Table 3). However, the comparisons of Table 3 depend on the assumption of constancy of staurolite Al_2O_3 and SiO_2 contents. In addition, it seems that there may have been a tendency for wet-chemical methods to underestimate Al_2O_3 and overestimate SiO_2. The proposed corrections bring the two high-quality Juurinen wet-chemical analyses into agreement with the present results on the same staurolites (Table 2).

RESULTS

The corrected analyses, including H_2O (Holdaway et al., 1986), and Li_2O and F (Dutrow et al., 1986), are given in Table 4 along with the stoichiometric amounts of the elements and the unit-cell dimensions. The average formula for these 31 staurolite specimens is $H_{3.2}R_{4.1}^{2+}Li_{0.2}Ti_{0.1}Al_{17.8}Si_{7.7}O_{48}$. Table 5 gives the range, average, standard deviation, and analytical precision for each element in terms of stoichiometry. The last column gives a measure of the amount of real variability in each element: the square root of the actual variance less the analytical variance (σ*). Some general observations based on Tables 4 and 5 are as follows: (1) The elements Si, Al, Ti, and Mn are very nearly constant in these staurolites, the maximum variation of σ* being 0.14 ions per formula unit (pfu) for Al, corresponding to ≤1% real variation. (2) The elements Fe, Mg, Zn, Li, and H all show wide ranges of relative variation, with σ* between 0.27 and 0.37 ions pfu, amounting to ≥11% of the average amount of the element. (3) Distributions of Zn and Li are highly skewed with low values in most staurolites, but with a few staurolites containing up to 1.32 and 1.39 ions pfu, respectively; no other elements show such strikingly skewed distributions. (4) The contents of R^{2+} and (R^{2+} + Li) show a systematic decrease as H increases; such effects are not seen for other elements.

In order to quantify some of the effects summarized above and learn more about the crystal chemistry of staurolite, we have grouped together elements that might be expected to show solid solution (Table 5). Each time an element is added to a group, a reduction in σ* indicates that the element tends to substitute for one or more of the other elements in the group. If the addition of an element increases σ*, then it shows that the element at least in part substitutes for some element not in the group. Only when the lowest possible σ* has been achieved can the elements involved be considered a reasonable approximation of the ions that substitute for each other.

---

[1] Unless otherwise stated, all errors quoted are $N - 1$ weighting of one standard deviation of the population (1σ).

Table 4. Chemical analyses, atomic proportions, and unit-cell dimensions of staurolites whose localities are given in Table 1

	3-3	86	ER-70	M-29	EH-6	164	114-1	KF-9	655-1	53-2
SiO₂	27.22	27.29	26.97	26.95	27.13	27.26	27.15	27.49	27.38	26.82
Al₂O₃*	54.14	54.02	53.59	54.52	53.03	53.90	54.06	53.68	53.80	54.57
TiO₂	0.54	0.50	0.53	0.46	0.47	0.49	0.44	0.43	0.55	0.50
Cr₂O₃	0.09	0.05	0.06	0.05	0.06	0.07	0.05	0.07	0.07	0.08
V₂O₅	0.03	0.04	0.03	0.03	0.03	0.04	0.05	0.02	0.02	0.04
CoO	0.02	0.03	0.03	0.03	0.03	0.03	0.03	0.04	0.03	0.02
FeOᵗ**	14.06	14.55	14.93	14.42	12.79	13.95	14.41	13.75	14.62	14.70
MgO	1.89	1.55	1.62	1.68	4.02	1.63	1.34	2.61	1.45	1.46
MnO	0.48	0.16	0.28	0.30	0.11	0.20	0.07	0.35	0.07	0.23
ZnO	0.18	0.28	0.27	0.16	0.30	0.23	0.29	0.10	0.25	0.24
Li₂O	n.d.	0.20	0.10	n.d.	0.01	0.18	0.37	0.12	0.17	0.23
H₂O	1.43	1.45	1.48	1.50	1.52	1.55	1.55	1.58	1.59	1.59
F	n.d.	0.01	0.01	n.d.	0.01	0.01	0.01	0.02	0.00	0.01
Total†	100.10	100.15	99.90	100.10	99.51	99.56	99.84	100.25	100.00	100.51
				Atomic proportions on the basis of 48 oxygens						
Si	7.638	7.657	7.609	7.562	7.616	7.664	7.621	7.671	7.679	7.498
Al	17.911	17.868	17.824	18.034	17.549	17.865	17.891	17.660	17.789	17.986
Ti	0.114	0.106	0.112	0.097	0.099	0.104	0.093	0.090	0.116	0.105
Cr	0.020	0.011	0.013	0.011	0.013	0.016	0.011	0.015	0.016	0.018
V	0.006	0.007	0.006	0.006	0.006	0.007	0.009	0.004	0.004	0.007
Co	0.005	0.007	0.007	0.007	0.007	0.007	0.007	0.009	0.007	0.004
Fe	3.300	3.414	3.523	3.384	3.003	3.280	3.383	3.209	3.429	3.437
Mg	0.790	0.648	0.681	0.702	1.682	0.683	0.561	1.085	0.606	0.608
Mn	0.114	0.038	0.067	0.071	0.026	0.048	0.017	0.083	0.017	0.054
Zn	0.037	0.058	0.056	0.033	0.062	0.048	0.060	0.021	0.052	0.050
Li	—	0.226	0.113	—	0.011	0.204	0.418	0.135	0.192	0.259
H	2.677	2.714	2.786	2.808	2.846	2.907	2.903	2.941	2.975	2.966
F	—	0.009	0.009	—	0.009	0.009	0.018	0.018	0.000	0.009
				Lattice parameters						
No. peaks	50	64	42	53	60	49	30	43	57	46
a (Å)	7.870(1)	7.872(1)	7.863(2)	7.870(1)	7.880(1)	7.873(1)	7.871(1)	7.872(1)	7.872(1)	7.872(1)
b (Å)	16.626(2)	16.622(2)	16.624(2)	16.618(2)	16.632(1)	16.614(2)	16.611(1)	16.619(2)	16.625(1)	16.620(2)
c (Å)	5.662(1)	5.659(1)	5.657(1)	5.659(2)	5.659(1)	5.563(1)	5.652(1)	5.658(1)	5.658(1)	5.662(1)
V (Å³)	740.8(1)	740.5(1)	739.5(1)	740.0(1)	741.7(1)	739.4(1)	739.0(9)	740.2(2)	740.5(1)	740.9(1)

* Systematic errors corrected—Al₂O₃ × 0.987, FeO × 1.04 (see text). FeOᵗ = total Fe as FeO.
** Li₂O and F assumed to be same as for PF-2 from the same locality.
† Total corrected for O = F, total includes ZrO₂.
‡ Unit-cell dimensions determined by D. T. Griffen, Brigham Young University.

Although this is a useful procedure for minerals that contain several ions substituting on several sites, it has the disadvantage that it cannot be used to demonstrate with certainty that a given ion substitutes in more than one group. However, σ^* close to zero for a group would indicate that the ions belong domminantly to that group.

When all the available analyses are considered, the elements fall into two fairly well defined groups: (Si + Al) with $\sigma^* = 0.09$ and (R²⁺ + ½H + Li) with $\sigma^* = 0.13$. Neither Mn nor Ti shows enough range in composition to allow it to be assigned to a group. However, Mn was assigned to the second group because of the probability that it substitutes for Fe (Smith, 1968). The trivial amount of F may be grouped with H, based on the inference that F replaces OH. These results suggest that to a first approximation Si and Al substitute for each other on one (or more) sites, and the R²⁺ ions, H, and Li substitute for each other on another group of sites.

If these two groups of ions adequately explained all chemical substitution, σ^* would approach zero for each group, assuming that random errors have been compensated by the correction for analytical precision. The fact that σ^* does not drop to zero for either group of ions

indicates that there is some degree of crossover of ions between the groups. There are at least four crystallochemically reasonable ways whereby this may happen:

1. Some Mg may replace Al on one or more sites. This has been proposed by most previous workers who have considered the crystal chemistry of staurolite. Our results show that because Mg increases σ^* for (Si + Al) and decreases σ^* for (R²⁺ + ½H + Li) and because the σ^* values for each group are on the order of 0.1 ion pfu, very little Mg ion replaces Al.

2. Some Al may replace R²⁺ on one or more sites. This type of substitution has also been proposed by most previous workers. A small amount of Al substituting for R²⁺ cannot be excluded on the basis of our analytical results.

3. Some Fe, probably in the form of Fe³⁺, may replace Al on one or more sites. Figure 1 shows that a significant amount of the variation of Al is caused by staurolite from three specimens, EH-6, M-1, and PF-3. Staurolite EH-6 coexists with magnetite, and the ilmenite composition of the other two specimens is not known. The issue is further clouded by the fact that three other specimens have staurolite with normal Al that coexists with ilmenite-hematite solid solution. If EH-6, M-1, and PF-3 are excluded,

Table 4—*Continued*

SL-2	356-1	SL-1	106038	117183	36764	CT-DL-1	M-1	117189	119551	78332
27.30	27.46	27.19	26.90	27.56	27.46	27.53	27.45	27.46	27.50	27.39
54.13	53.42	54.58	54.56	53.93	53.93	53.50	52.50	52.94	53.15	53.82
0.45	0.52	0.54	0.38	0.62	0.56	0.56	0.50	0.53	0.70	0.49
0.05	0.05	0.02	0.05	0.10	0.04	0.05	0.06	0.06	0.08	0.07
0.06	0.03	0.08	0.03	0.03	0.06	0.06	0.03	0.04	0.05	0.04
0.02	0.03	0.02	0.02	0.02	0.03	0.03	0.02	0.02	0.03	0.02
14.16	14.65	13.56	10.37	13.88	14.00	14.51	14.78	9.13	13.85	14.21
1.84	1.65	1.79	2.63	2.17	1.74	1.53	2.58	1.93	2.39	1.53
0.02	0.05	0.01	0.36	0.22	0.14	0.03	0.13	0.15	0.10	0.08
0.19	0.23	0.18	3.05	0.23	0.18	0.20	0.34	6.33	0.15	0.11
0.11	0.11	0.37	0.01	0.01	0.13	0.16	0.07	0.05	0.03	0.11
1.60	1.60	1.63	1.62	1.63	1.63	1.63	1.65	1.65	1.73	1.75
0.02	0.01	0.02	0.02	0.01	0.01	0.01	0.01	0.01	0.01	0.02
99.96	99.81	100.07	99.99	100.43	99.97	99.84	100.12	100.33	99.78	99.64
			Atomic proportions on the basis of 48 oxygens							
7.641	7.717	7.577	7.525	7.679	7.682	7.725	7.712	7.734	7.700	7.677
17.860	17.699	17.931	17.994	17.715	17.788	17.699	17.388	17.579	17.545	17.783
0.095	0.110	0.113	0.080	0.130	0.118	0.118	0.106	0.112	0.147	0.103
0.011	0.011	0.004	0.011	0.022	0.009	0.011	0.013	0.013	0.018	0.016
0.011	0.006	0.015	0.006	0.006	0.006	0.011	0.011	0.007	0.009	0.007
0.004	0.007	0.004	0.004	0.004	0.007	0.007	0.005	0.005	0.007	0.004
3.314	3.443	3.160	2.426	3.234	3.276	3.405	3.473	2.151	3.243	3.331
0.767	0.691	0.743	1.096	0.901	0.725	0.640	1.080	0.810	0.997	0.639
0.005	0.012	0.002	0.085	0.052	0.033	0.007	0.031	0.036	0.024	0.019
0.039	0.048	0.037	0.630	0.047	0.037	0.041	0.071	1.316	0.031	0.023
0.124	0.124	0.415	0.011	0.011	0.146	0.181	0.079	0.057	0.034	0.124
2.988	3.000	3.031	3.023	3.030	3.043	3.052	3.092	3.100	3.232	3.272
0.018	0.009	0.018	0.018	0.009	0.009	0.009	0.009	0.009	0.009	0.018
			Lattice parameters							
54	52	67	56	55	43	43	51	60	59	42
7.871(1)	7.860(2)	7.872(1)	7.872(1)	7.870(1)	7.860(2)	7.866(1)	7.877(1)	7.865(1)	7.869(1)	7.868(1)
16.617(1)	16.620(2)	16.601(1)	16.604(3)	16.616(2)	16.617(3)	16.623(1)	16.631(2)	16.606(1)	16.627(2)	16.615(2)
5.656(1)	5.653(1)	5.655(1)	5.655(1)	5.660(1)	5.660(1)	5.654(1)	5.661(1)	5.656(1)	5.658(1)	5.656(1)
739.8(1)	739.5(1)	739.1(1)	739.1(1)	740.1(1)	739.3(2)	739.3(1)	741.5(1)	738.8(1)	740.3(1)	739.4(2)

(Si + Al) for the remaining staurolites changes from 25.43 ± 0.13 to 25.46 ± 0.09. If only those staurolite specimens known to have crystallized under very reducing conditions with graphite and hematite-free ilmenite (four specimens studied by Holdaway and Dutrow, in prep., and two specimens studied by Guidotti, 1974; all from Maine) are averaged, (Si + Al) is 25.53 ± 0.03. This provides some indication that Fe^{3+}, which should be higher in staurolites that grew under oxidizing conditions, substitutes for Al (or perhaps Si).

4. Still another cause of minor crossover between groups is the substitution involving Li. If this substitution involves Al, then presence of Li must increase σ^* for (Al + Si). This is discussed below and by Dutrow et al. (1986).
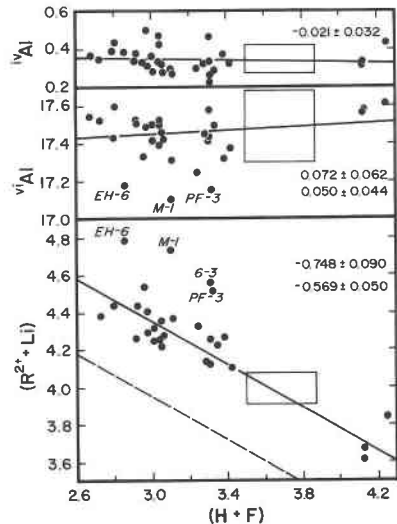
→

Fig. 1. Linear regressions (York, 1966) of stoichiometric (H + F) vs. ^{iv}Al, (H + F) vs. ^{vi}Al, and (H + F) vs. (R^{2+} + Li). ^{vi}Al is given by (Al + Si − 8), and it is assumed that replacement of ^{iv}Fe ions by Al is negligible. Slope of regression lines is indicated on each plot. Box indicates 2σ analytical error for each data point. First slope is value based on all data points; second value excludes marked points that may be high in Fe^{3+} or inaccurate in Li

(6-3, Dutrow et al., 1986). Regression lines plotted are those of the second determination. For (H + F) vs. (R^{2+} + Li), the dashed line is 0.4 (R^{2+} + Li) ions below the regression line. It represents the expected ^{iv}Fe-site content, after allowing for 0.25 (Mn + Fe^{2+}) in U(1), 0.25 Fe^{3+} in Al(3A) and 0.1 Ti in ^{iv}Fe.

Table 4—*Continued*

	6-3	B14040**	GTU-104	PF-3**	355-1	PE-1	PF-2	77-55C	71-60E	71-62R
SiO_2	28.36	27.62	26.94	27.58	27.59	27.26	27.62	27.62	27.79	27.79
Al_2O_3*	55.04	54.22	54.31	52.72	53.88	53.62	54.03	55.88	54.88	54.95
TiO_2	0.40	0.61	0.42	0.55	0.40	0.65	0.66	0.35	0.43	0.43
Cr_2O_3	0.10	0.04	0.02	0.05	0.06	0.08	0.05	n.d.	0.07	0.05
V_2O_5	0.03	0.04	0.02	0.03	0.03	0.05	0.05	n.d.	0.02	0.04
CoO	0.02	0.02	0.09	0.03	0.03	0.03	0.03	n.d.	0.04	0.03
FeO'*	10.88	13.03	9.42	14.30	14.37	14.26	13.18	13.60	12.64	12.83
MgO	0.91	2.24	1.98	2.25	1.10	1.72	2.14	0.18	0.79	0.69
MnO	0.43	0.21	0.29	0.43	0.12	0.07	0.18	0.12	0.34	0.23
ZnO	0.99	0.29	5.26	0.25	0.25	0.25	0.23	0.03	0.09	0.24
Li_2O	1.26	0.06	0.05	0.06	0.29	0.13	0.06	0.56	0.24	0.29
H_2O	1.80	1.78	1.77	1.77	1.78	1.81	1.84	2.24	2.25	2.26
F	0.02	0.01	0.01	0.01	0.02	0.01	0.01	0.18	0.02	0.01
Total	100.23	100.19	100.66	100.03	99.91	99.94	100.08	100.68	99.59	99.85
Atomic proportions on the basis of 48 oxygens										
Si	7.781	7.669	7.533	7.730	7.713	7.627	7.674	7.566	7.686	7.674
Al	17.802	17.749	17.903	17.421	17.757	17.686	17.699	18.046	17.895	17.890
Ti	0.083	0.127	0.088	0.116	0.084	0.137	0.138	0.072	0.089	0.089
Cr	0.022	0.009	0.004	0.011	0.013	0.018	0.011	—	0.015	0.011
V	0.005	0.007	0.004	0.006	0.006	0.009	0.009	—	0.004	0.009
Co	0.004	0.004	0.020	0.007	0.007	0.007	0.007	—	0.009	0.007
Fe	2.496	3.026	2.203	3.352	3.360	3.337	3.063	3.116	2.924	2.963
Mg	0.372	0.927	0.825	0.940	0.458	0.717	0.887	0.073	0.326	0.284
Mn	0.100	0.049	0.069	0.102	0.028	0.017	0.042	0.028	0.080	0.054
Zn	0.201	0.059	1.086	0.052	0.052	0.052	0.047	0.006	0.018	0.049
Li	1.391	0.067	0.056	0.068	0.326	0.146	0.067	0.617	0.267	0.322
H	3.294	3.297	3.302	3.310	3.320	3.378	3.411	4.093	4.152	4.164
F	0.017	0.009	0.009	0.009	0.018	0.009	0.009	0.156	0.017	0.009
Lattice parameters										
No. peaks	54	59	45	58	60	70	67	55	43	54
a (Å)	7.868(1)	7.878(1)	7.869(1)	7.875(1)	7.872(1)	7.874(1)	7.874(1)	7.867(2)	7.850(2)	7.870(1)
b (Å)	16.594(2)	16.623(1)	16.603(2)	16.632(1)	16.624(2)	16.628(1)	16.617(2)	16.607(3)	16.611(2)	16.608(3)
c (Å)	5.656(1)	5.656(1)	5.656(1)	5.662(1)	5.652(1)	5.659(1)	5.657(1)	5.653(1)	5.652(1)	5.648(1)
V (Å³)	738.4(1)	740.7(1)	738.9(1)	741.5(1)	739.6(1)	740.9(1)	740.1(1)	738.5(2)	737.0(1)	738.3(2)

Whereas minor crossover of Al and Mg between the two groups is possible, the present model excludes this possibility in order to provide enough constraints to unequivocally assign elements to each site.

The near constancy of the sum (R^{2+} + Li + ½H) provides a basis for determining the substitution responsible for variable H or (H + F). Without going into details of the staurolite structure at present, the main possibilities for this substitution are vacancy substitutions involving ^{iv}Al, ^{vi}Al, or (R^{2+} + Li) (see also Lonker, 1983). Figure 1 shows plots of (H + F) against these ions along with the results of linear regression that allow for errors in both x and y (York, 1966). ^{iv}Al is of necessity defined as (8 − ^{iv}Si) and involves the assumption that the ^{iv}Si sites are filled with only Si and Al. ^{vi}Al is defined as (Al + Si − 8) to be consistent with the present model. Regressions for ^{vi}Al and (R^{2+} + Li) against (H + F) are given both with and without the identified points that may be high in Fe^{3+}, and therefore low in ^{vi}Al, or that may have inaccurate analyses of Li (e.g., specimen 6-3). The slopes of the ^{iv}Al and ^{vi}Al regressions are near zero. Proposed substitutions should give a negative slope for ^{iv}Al or ^{vi}Al. The (H + F) vs. (R^{2+} + Li) regression has a slope of −0.57 if the identified points are excluded. Substitutions that involve H create the necessity for charge balance as metal ions cannot directly replace H. An (R^{2+} + Li) substitution

for H should give a slope of −0.5, close to the observed slope. A proposed substitution of Li + $\frac{1}{3}^{vi}Al$ ⇌ R^{2+} + ⅓□ (Dutrow et al., 1986) accounts for the charge difference between R^{2+} and Li. Consequently, the most important substitution to explain variable H is 2H ⇌ (R^{2+} + Li).[2]

CRYSTAL-CHEMICAL MODEL

Structure

The structure refinement by Smith (1968) was done on Pizzo Forno staurolite, very similar to B14040. The recent determination of Tagai and Joswig (1985) on a staurolite from the same locality leads to very similar results. The kyanite layer is composed of 8 Si tetrahedra, 4 Al(1A) octahedra, 4 Al(1B) octahedra, and 8 Al(2) octahedra (site nomenclature from Smith, 1968). The iron hydroxide layer (Fig. 2) contains partially occupied Al(3A) and Al(3B) octahedra, partially occupied Fe tetrahedra, and slightly occupied U(1) and U(2) octahedra. According to Takéuchi et al. (1972) and Tagai and Joswig (1985), the H sites P(1A) and P(1B) are located on the faces of the Al(3A)

---

[2] Here and elsewhere in this report the grouping of ions in parentheses in a substitution scheme indicates ions that reside on a single site. Ions not in parentheses but on the same side of the equation reside on different sites.

Table 5. Range, average, and standard deviation of ions and groups of ions for 31 staurolite analyses, based on 48 oxygens

Element(s)	Range	Average	Std. dev.	Analytical precision	$\sqrt{\Delta\sigma^2}$*
Si	7.50–7.78	7.65	0.07	0.04	0.06
Al	17.39–18.05	17.78	0.17	0.09	0.14
Si + Al	25.10–25.61	25.43	0.13	0.10	0.09
Si + Al**	25.25–25.61	25.46	0.09	0.10	0.00
Si + Al + Mg†	25.68–26.85	26.17	0.22	0.10	0.20
Ti	0.07–0.15	0.11	0.03	0.01	0.02
Fe	2.15–3.52	3.15	0.36	0.03	0.36
Zn	0.01–1.32	0.14	0.30	0.01	0.30
Mn	0.00–0.11	0.05	0.03	0.01	0.03
Mg	0.07–1.68	0.74	0.29	0.01	0.29
Li‡	0.01–1.39	0.22	0.27	0.02	0.27
H	2.68–4.16	3.17	0.38	0.09	0.37
R^{2+}§	3.17–4.77	4.08	0.37	0.03	0.37
R^{2+} + H	6.46–7.76	7.24	0.28	0.10	0.26
R^{2+} + ½H	4.82–6.21	5.66	0.27	0.08	0.25
R^{2+} + H + Li‡	7.11–7.93	7.47	0.23	0.10	0.21
R^{2+} + ½H + ½Li‡	5.52–6.21	5.77	0.18	0.08	0.16
R^{2+} + ½H + Li‡	5.69–6.28	5.88	0.15	0.08	0.13
R^{2+} + ½H + ½F + Li**,‡,‖	5.70–6.02	5.85	0.10	0.08	0.06
Fe + Zn + Mn + ½H + Li†,‡	4.52–5.84	5.14	0.28	0.06	0.27

* $\sqrt{\Delta\sigma^2}$ (σ* in text) is the square root of the difference between variances of analytical data and analytical precision, the squares of entries in the previous two columns. σ* gives a measure of the real variation, in ions per formula unit, of each element or group of elements.
** Excluding three analyses (EH-6, M-1, and PF-3) that may have high Fe^{3+} (see Fig. 1 and text).
† Compare with listing two lines above to determine effect of reassigning Mg to other group.
‡ Based on the 29 specimens for which Li is available.
§ R^{2+} includes Fe^{3+} since Fe_2O_3 was not analyzed separately.
‖ Excluding 6-3, believed to be inaccurate owing to variability in Li (Dutrow et al., 1986).

and Al(3B) octahedra near O(1A) and O(1B) and about midway between Al and Fe sites (Fig. 3).

Donnay and Donnay (1983) have emphasized the fact that most, or perhaps all, staurolites are truly monoclinic. The monoclinic character results from small differences in the sizes (and perhaps the occupancies) of the Al(1A) and Al(1B), Al(3A) and Al(3B), and U(1) and U(2) octahedra, and from different site occupancies of the Al(3A) and Al(3B), and U(1) and U(2) octahedra (Smith, 1968).

Smith has shown that the occupancy at Al(3A) is about 1.5 times that at Al(3B) and the occupancy at U(1) is about twice that at U(2), findings consistent with partial order on those sites. Tagai and Joswig (1975) show comparable features. Smith (1968) also suggested the possibility that Al(3B) and U(2) are empty, and the observed occupancy results from twinning on (001). On the basis
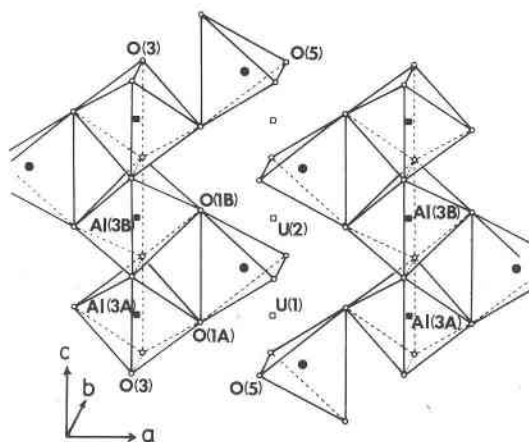

Fig. 2. Structure of the iron hydroxide layer of staurolite showing locations of the ions. In the present model, Al(3B) is always vacant. Modified slightly after Ward (1984a).
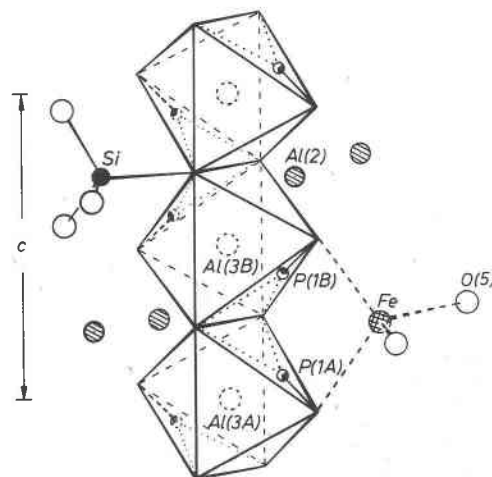

Fig. 3. Structure of part of the iron hydroxide layer to show the H locations, P(1A) and P(1B). In the present model P(1A) is occupied only when the adjacent Al(3A) and ^{iv}Fe sites are vacant. After Takéuchi et al. (1972).

Table 6. Comparison of site occupancies for staurolite from Pizzo Forno (probably similar to B14040)

Site	Multi-plicity	Occupancy (%) Smith (1968)	Occupancy (%) (present model)
		Kyanite layer	
Si	8	93Si, 6Al, 1□	96Si, 4Al
Al(1A)	4	93Al, 5Mg, 2□	100Al
Al(1B)	4	93Al, 5Mg, 2□	100Al
Al(2)	8	93Al, 5Mg, 2□	100Al
		Iron hydroxide layer	
^{iv}Fe	4	59Fe, 29Al, 4Ti, 8□	64Fe, 23Mg, 3Ti, 2Li, 1Zn, 7□
Al(3A)	2	28Al, 14Fe, 58□	68Al, 13Fe^{3+}, 19□
Al(3B)	2	19Al, 9Fe, 72□	—
U(1)	2	5Fe, 3Mn, 92□	10Fe, 2Mn, 88□
U(2)	2	3Fe, 1Mn, 96□	
P(1A)	4	38H,* 62□	7H,** 93□
P(1B)	4	48H,* 52□	76H, 24□

* Tagai and Joswig (1985) on staurolite from the same locality.
** 7% H are assigned to the P(1A) site to provide one-half of the charge balance for the 7% tetrahedral vacancies, as discussed in the section on bond-valence calculations.

of this and the observation of antiphase domain boundaries in some staurolites (Fitzpatrick, 1976), Ribbe (1982) suggested that ordering has occurred on these two pairs of sites at some time after initial crystallization. Another argument in favor of some kind of twinning is that the occupancies of the four sites involved are all ≤0.5, implying that they would be ≤1.0 if fully ordered. For the present model we assume an idealized, fully ordered staurolite of Pizzo Forno composition with Al(3A) and U(1) partially occupied and with Al(3B) and U(2) empty. At the other extreme, a disordered staurolite would be orthorhombic and have equivalent occupancy of Al(3A) and Al(3B), and of U(1) and U(2).

Fe oxidation state and site considerations

One aspect that the present study has not addressed is determination of Fe^{2+}/Fe^{3+} ratios of staurolites. Methods that involve small amounts of material (Fritz and Popp, 1985) have not yet been perfected for minerals as refractory as staurolite. At present we must depend on previous analytical studies and Mössbauer data. The best Fe^{2+}/Fe^{3+} determinations seem to be those of Juurinen (1956). Earlier analyses cited by Juurinen show, in some instances, what seem to be anomalously high Fe_2O_3 values coupled with low FeO and Al_2O_3. Juurinen's six analyses give a range of Fe_2O_3 from 0.84 to 1.47 wt% and average 1.11%, corresponding to 0.18 to 0.31 Fe^{3+} ions pfu and averaging 0.23 ions pfu.

Mössbauer studies show that most Fe is Fe^{2+}, mostly on one site, with minor amounts of Fe^{3+}. From Mössbauer studies of Pizzo Forno staurolite (probably B14040), Smith (1968) concluded that most of the Fe was Fe^{2+} and at the ^{iv}Fe site, but that about 23% of the Fe occurs at one or two other sites. Bancroft et al. (1967) assigned two Fe doublets to a dominant tetrahedral and minor distorted octahedral site. Dowty (1972) suggested that the great tem-

perature dependence of the weaker doublet implied that it also was due to a tetrahedral site, possibly the result of positional disorder at the ^{iv}Fe site (Smith, 1968). Scorzelli et al. (1976) also found evidence for two doublets, both of which were interpreted to be due to Fe^{2+}. Regnard (1976) interpreted Mössbauer results to indicate Fe^{2+} at two distorted octahedral sites besides the ^{iv}Fe site; he also cited evidence that 2–3% of the Fe was Fe^{3+} in his staurolite. Dickson and Smith (1976) concluded that some Fe must be at sites other than the ^{iv}Fe site. Finally, Warren Thomas (1984, pers. comm.) has done Mössbauer studies of staurolite 77-55c and has suggested that 5 ± 3 wt% Fe_2O_3 exists in this specimen.

We conclude from Juurinen's analyses and the Mössbauer studies that Fe in staurolite is dominantly Fe^{2+}, but amounts of Fe^{3+} between 0.2 and 0.3 ions pfu exist in normal staurolites. Most of the Fe is tetrahedral and occupies the ^{iv}Fe site; however, small amounts of octahedral Fe exist in as many as two other sites, presumably the Al(3A) and U(1) sites. On the basis of the present work, an argument may be made to support the assignment of most or all Fe^{3+} to the Al(3A) site. Three analyses with high $(R^{2+} + Li)$ (Fig. 1) have these high values mirrored by low ^{vi}Al (defined as Al + Si − 8). For EH-6, M-1, and PF-3, the $(R^{2+} + Li)$ values fall an average of about 0.35 ions above the regression line based on the other analyses, whereas for the same staurolites, ^{vi}Al falls an average of 0.30 ions below the ^{vi}Al line. This can possibly be explained by substitution of 0.30 to 0.35 ^{vi}Al ions by Fe^{3+}, which would be seen as part of the $(R^{2+} + Li)$ component. Al(3A) is a possible site for the substitution since it is the largest octahedral Al site (Smith, 1968).[3] The remaining staurolites should have an average of about 0.25 Fe^{3+} ions, whereas these three possible Fe^{3+}-rich staurolites may have an average of 0.55 to 0.60 Fe^{3+} ions in total. Alternative explanations for the scatter in Figure 1 are (1) the ^{iv}Fe and ^{vi}Al sites each have a range of occupancies or (2) a small amount of Mg exists at ^{vi}Al sites. The fact that only three staurolites have high $(R^{2+} + Li)$ and low ^{vi}Al and the rest are much more consistent with each other does not lend support to these possibilities. However, the possibility of some Mg in the ^{vi}Al sites cannot be ruled out.

Site occupancies

On the basis of the foregoing discussion, the chemical analysis of staurolite B14040, and the data of Table 5, we have reinterpreted Smith's (1968) site occupancies in such a way as to be as consistent as possible with the observed scattering factors and cation–oxygen distances. Table 6 is a comparison of the present model with that of Smith. An approximate site scattering factor may be calculated by summing the percentage of each ion times its number of electrons (an average of the atom and the ion was used). The two models produce site scattering factors within about

---

[3] The slightly larger Al(3B) site would also be a candidate for Fe^{3+}. However, for the present model, we assume an idealized fully ordered staurolite with Al(3B) empty.

Table 7. Average cation–oxygen distances for staurolite B14040, in ångströms

Site/Coord.		Mean distance (Smith, 1968)	Kyanite (Winter and Ghose, 1979)		Present model*		Distances for suggested ions[a]		
					Pred.	Meas.	Ion	Tet.	Oct.
Kyanite layer							Si	1.636[b]	—
							Al	1.763[b]	1.907[b]
Si	4	1.641	Si(1,2)	1.636[b]			Ti	1.825[c]	2.005
Al(1A)	6	1.911	Al(1)	1.902[b]			Fe^{3+}	1.895[c]	2.045
Al(1B)	6	1.914	Al(2)	1.913[b]			Mg	1.975[c]	2.12
Al(2)	6	1.907	Al(3,4)	1.907[b]			Zn	1.975[f]	2.14
Al(av.)	6	1.909		1.907[b]			Li	1.995[c]	2.16
Iron hydroxide layer							Fe^{2+}	2.035[c]	2.18
							Mn	2.065[c]	2.23
ivFe	4	2.008			(2.008)	2.008	□ivFe	1.95[g,h]	—
Al(3A)	6	1.973			1.947	1.939[d]	□Al(3A,B)	—	2.025[d,h]
Al(3B)	6	1.992			(2.025)	2.025[d]	□U(1,2)	—	2.161[e,h]
U(1)	6	2.165			2.164	2.167[e]			
U(2)	6	2.163			(2.161)	2.161[e]			

[a] From Shannon (1976) unless otherwise stated.
[b] Winter and Ghose (1979), kyanite; sillimanite for ivAl.
[c] Modified specifically for the ivFe site, Shannon (1976) values increased by 0.025, see text.
[d] Linear extrapolation of Smith (1968) distances to all ions in 3A site and no ions in 3B site, using present model for occupancies (Table 6).
[e] Linear extrapolation of Smith (1968) distances to all ions in U(1) and no ions in U(2), using present model for occupancies (Table 6).
[f] Griffen (1981) average values increased by 0.025, see text.
[g] Estimated as the value needed to bring mean tetrahedral radius cubed of low-R^{2+} staurolites into agreement with that of other staurolites (Fig. 4).
[h] These values must be regarded as approximate.
* ( ) Predicted and measured values agree because of method of calculating vacancy size or ionic radius.

3% or less of each other. The Al sites in the kyanite layer are 2.3% higher in the present model, indicating that a few sites are vacant or filled by a lighter element such as Mg. Occupancy of the Fe site is 3.4% higher in this model, suggesting the possibility of slightly less Fe at that site.

Table 7 provides (1) the mean cation–oxygen distances for the various sites in staurolite (Smith, 1968); (2) the mean cation–oxygen distances for kyanite (Winter and Ghose, 1979) for comparision with those distances for the kyanite layer of staurolite; (3) predicted cation–oxygen distances based on the present model and tabulated cation–oxygen distances of Shannon (1976) and other sources as indicated; and (4) measured cation–oxygen distances based on Smith's (1968) values and the present model, which assumes all Al(3) ions are at Al(3A) and all U(1,2) ions are at U(1). A 4% substitution of ivSi by ivAl (Table 6) may explain the slightly larger size of the ivSi site than in kyanite. The average Al–O distance in the kyanite layer of staurolite is almost identical to that of kyanite, supporting the idea that the 16 kyanite-layer octahedra contain almost entirely Al. Comparison of the remaining cation–oxygen distances with predicted values requires estimates of the size of a vacancy for each site. These distances were estimated for Al(3B) and U(2) by linear extrapolation of Smith's Al(3A) and Al(3B), and U(1) and U(2) distances to zero occupancy. The approximate cation-oxygen distances for vacancies are 2.03 and 2.16 Å, respectively.

The vacancy size at the ivFe site is difficult to assess. However, even a rough estimate of the size of tetrahedral vacancies has considerable importance regarding staurolite crystal chemistry and petrology. The mean cation-oxygen distance for the site is almost exactly the same as

the Shannon (1976) tetrahedral Fe^{2+}–O distance. If we make the tenuous assumption that tetrahedral radii can be used to approximately predict bond lengths for the ivFe site, the large amount of smaller ions, Mg, Zn, Li, and possibly Ti would imply that the vacancy size should be substantially larger than the size of Fe^{2+} (~2.5 Å) for the ~7% vacancies in the Pizzo Forno staurolite. On the other hand, the fact that the ions in the site have cation–anion distances of 2 Å or less is inconsistent with such a large size for vacancies. Perhaps more important, the r^3 values, where r is the mean ivFe-site ionic radius, for the three staurolites with lowest (R^{2+} + Li) are significantly higher than those for other staurolites (Fig. 4). These three staurolites have tetrahedral vacancies between 14 and 20%. One way to bring these trends into agreement is to allow for vacancies substantially smaller than the average size of the site. When the tetrahedral vacancies are included at a cation–oxygen distance of 1.95 Å ($r = 0.57$ Å), the two groups approximately coincide. A vacancy size larger than this value would increase the mean r^3 values so that they would fall well to the right of the main trend in Figure 4. Thus a vacancy about the same size as the smaller ions is needed to account for the cell dimensions of low-R^{2+} staurolites. Inspection of Figure 4 shows that a vacancy radius of 0.57 is the *maximum* possible value. This effect is largely independent of the actual cation–oxygen distances (or radii) assumed for the ions. It is reasonable to expect that tetrahedral vacancies should be smaller than tetrahedral Fe^{2+}, because putting the large Fe^{2+} ion into tetrahedral coordination requires local distortion of the close-packed oxygen array to make room for it. Replacing some O by OH is not expected to have a measurable effect on the unit-cell volume.
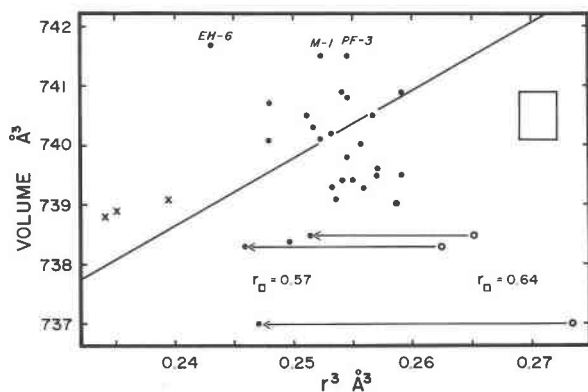
Fig. 4. Unit-cell volume for staurolites of this study plotted against r^3 (r = mean ^{iv}Fe-site ionic radius). In order to determine tetrahedral occupancy, 0.25 (Mn + Fe^{2+}) was subtracted from total (R^{2+} + Li) to allow for U(1) occupancy, and 0.25 Fe^{3+} was subtracted for Al(3A) occupancy. Mg, Zn, Li, and Ti were assigned to the ^{iv}Fe site plus the remaining Fe. Radii are those of Table 7 (cation–oxygen distance less 1.38 equals radius; Shannon, 1976). Three high-Zn staurolites are indicated by crosses, and labeled points correspond to staurolites that may have high Fe^{3+}. Solid line corresponds to the regression of r^3 vs. V given by Griffen (1981). Open circles are low-R^{2+} staurolites that plot at high values of r^3 when the contribution of tetrahedral vacancies is ignored, equivalent to assuming that vacancies have the same size as the mean radius of ^{iv}Fe-site ions. The value used for radius of vacancies for all staurolites represented by closed circles or crosses (0.57 Å), is the maximum possible value, which brings r^3 for low-R^{2+} staurolites to the edge of the scatter. Box indicates approximate 2σ error. Scatter results from variable Fe^{3+}, inaccuracies in the method of assigning ions to the ^{iv}Fe site, and minor contributions from less-variable sites.

This small size for a tetrahedral vacancy suggested by the unit-cell dimensions results in a low value of mean cation–oxygen distance if it is estimated by a linear combination of average tetrahedral cation–oxygen distances of Shannon (1976) combined with ~1.95 Å for vacancies. Shannon bond lengths may be adapted for this specific site by increasing all the cation–oxygen distances by 1.25%, increasing ionic radii of ^{iv}Fe, ^{iv}Mg, ^{iv}Zn; and ^{iv}Li by a value of 0.025 Å. In addition, a range of values is to be expected from bond-strength considerations (Brown, 1981). It is reasonable that the measured size of this site in staurolite should be larger than predicted from Shannon bond lengths when one considers that Smith (1968) has shown substantial positional (or temporal) disorder for this site. The modified cation–oxygen distances are given in Table 7. Minor considerations such as the location of the Ti, Fe^{3+}, and Mn ions have an insignificant effect on these conclusions. However, because a constant value of 0.25 Fe^{3+} ions in Al(3A) was assumed for Figure 4, variation in Fe^{3+} is expected to be an important contributor to the scatter in the plot. Assignment of any Al to the ^{iv}Fe site, possibly in place of Mg, would necessitate still larger sizes for the other ions.

Ti is tentatively placed at the ^{iv}Fe site following the suggestion of Ward (1984b) based on spectroscopic evidence. However, it should be pointed out that Donnay and Donnay (1983) have suggested that both Ti and Al have radii too small for the ^{iv}Fe site. Study of Ward's analyses from a single variable Ti staurolite suggests that charge balance may be maintained by decreased Al in Al(3A) in the same way as seems to happen for Li (Dutrow et al., 1986). An alternative site for Ti is Al(3A), but assignment of Ti to this site would necessitate removal of some Fe^{3+} in order to explain the observed site occupancy. Following Smith (1968), larger Mn^{2+} and Fe^{2+} ions are placed at U(1) sites. The modified cation–oxygen distances of ions assigned to the ^{iv}Fe site range from 1.825 to 2.035 Å. It is worth noting that Ti, the smallest of these, is always a minor constituent, whereas Mn, the largest U-site ion, is also very minor in amount.

The grouping of R^{2+} and Li ions at the ^{iv}Fe and U sites and of all Al in the kyanite layer and Al(3A) sites requires further discussion. In his structure determination, Smith (1968) assigned all Mg to kyanite-layer octahedral sites and a comparable amount of Al to the ^{iv}Fe sites. However, he pointed out that the very similar scattering factors of Al and Mg made the assignment somewhat arbitrary. On the basis of microprobe analyses and principal-component analysis of the data, Griffen and Ribbe (1973) proposed similar substitutions. Their stoichiometries were based on a fixed H content of 4. We believe this fixed H, and the absence of Li analyses, may have created artificial correlations between elements. The same kind of artificial correlation is seen between (Al + Si − 8) and (Fe + Mg + Zn) in the more recent study of Griffen et al. (1982). The present results show that (Al + Si − 8) is nearly constant for staurolites (17.43 ± 0.13, Table 5) when H and Li are analyzed and taken into account in the stoichiometry. The data of Tables 4 and 5 and the subsequent analysis given above show clearly that the ions Fe, Mg, Mn, Zn, and Li behave more or less as a group, and the limited variation in Al and Si is largely with respect to each other at the ^{iv}Si site. Additional supporting evidence comes from the fact that endmember staurolites have been synthesized with high yields and bulk compositions corresponding to 18 Al, 7.5 Si, and ~4 Fe (Richardson, 1968) ~4 Zn (Griffen, 1981), and ~4 Mg (Schreyer and Siefert, 1969) ions. Li must also be placed with these ions because its presence causes a decrease in R^{2+} (Table 4) and when it is grouped with R^{2+} ions (Table 5), the standard deviation of the group is reduced. These ions as a group are believed to occupy the ^{iv}Fe and U(1) sites.

Bond-valence calculations and vacancy distribution

Despite the re-assignment of cations and the assumption of ordering in staurolite, there are still vacancies possible for each site of the iron hydroxide layer (Fig. 2). Based on the present model for Pizzo Forno staurolite (Table 6), these are ^{iv}Fe—7%, Al(3A)—19%, P(1B)—24%, and U(1)—88%. Bond-valence calculations (Brown, 1981) can be useful in assigning cations to sites and, when cation assignments are known, in determining the relative positioning of vacancies. Brown's approach takes into ac-

Table 8. Bond-valence determinations for oxygen sites in staurolite

Cations	O(1A)	O(1B)[a]	Cations	O(3)[b]
None	0.97	0.96	None	1.50
U(1)	1.34	1.35	P(1A) or *P(1B)*	1.65[e]
ivFe	1.41	1.41[d]	P(1A), P(1B)	1.81[fg]
Al(3A)	1.56	1.54	Al(3B)	1.83
P(1A)	1.60[f]	1.60[fg]	Al(3A)	1.86[d]
U(1), ivFe	1.78[e]	1.79	Al(3B); *P(1A)* or P(1B)	1.99
U(1), Al(3A)	1.93	1.92	Al(3A); P(1A) or *P(1B)*	2.01[c]
U(1), P(1A)	1.97[g]	1.98	Al(3A), Al(3B)	2.19
ivFe, Al(3A)	2.00[cd]	1.98	Al(3A), Al(3B); P(1A) or P(1B)	2.35
ivFe, P(1A)	2.04	2.04[ce]	All	2.50
Al(3A), P(1A)	2.19	2.17		
U(1), ivFe, Al(3A)	2.37	2.37		
U(1), ivFe, P(1A)	2.41	2.43	Cations	O(5)
U(1), Al(3A), P(1A)	2.56	2.56		
ivFe, Al(3A), P(1A)	2.64	2.62	None	1.59[f]
All	3.01	3.00	U(2)	1.89
			U(1)	1.89[g]
O(2A)[b]		1.92[cdefg]	ivFe	2.13[cd]
			U(2), U(1)	2.19
O(2B)[b]		1.92[cdefg]	ivFe, U(2)	2.43
			ivFe, U(1)	2.43[e]
O(4)[b]		1.99[cdefg]	All	2.73

Note: Bond-valence sums for each oxygen site were determined using the method of Brown (1981). Every possible vacancy-occupancy configuration for the iron hydroxide layer is listed. Listings marked "none" include only bonds to fully occupied kyanite-layer ions, those marked "all" include all iron hydroxide–layer ions. Calculations were made using Si, Al, Fe^{2+}, and H. O(2A), O(2B), and O(4) are kyanite-layer oxygens. Cations listed are only those of the iron hydroxide layer. Italics refers to preferred site.

[a] Same combinations as O(1A) except U(1) is replaced by U(2), Al(3A) by Al(3B), and P(1A) by P(1B).

[b] Since 4% of ivSi is replaced by ivAl, all bond sums for O(2A), O(2B), O(3), and O(4) may be corrected for ivAl replacing ivSi by subtracting 0.24.

[c] Most common or "normal" configuration.

[d] Alternate "normal" configuration.

[e] Configuration with Al(3A) sites vacant.

[f] Configuration with ivFe sites vacant.

[g] Configuration with ivFe sites vacant and U(1) sites filled.

count bond length–bond valence considerations. The approach of determining which vacancy-occupancy combinations are most likely to occur leads directly to reasonable substitution models. Such information is important in determining activity models and disorder entropy.

Bond-valence values were calculated for all possible vacancy configurations (Table 8) using the cation–oxygen distances given by Smith (1968). These results must be regarded as approximate because of the probability of domain structure or disorder involving Al(3) sites that might be expected to make the O(1A) and O(1B) cation–oxygen distances seem more similar than in a fully ordered staurolite. Also, positional disorder at the ivFe site can be expected to change bond-valances to ivFe from O(1A), O(1B), and O(5) (Fig. 2).

The calculations show a wide range of possible bond-valence sums when all configurations are considered. Individual values that are far from 2 may be explained by (1) additional H sites (Donnay and Donnay, 1983); (2) disorder at a site; or (3) the nonoccurrence of that particular configuration. Bond-valence sums for oxygens in the kyanite layer vary from 1.92 to 1.99 and from 1.68 to 1.75 when ivAl occupies the ivSi site. Most bond-valence sums would be expected to lie between about 1.6 and 2.4. Thus it appears from Table 8 that with the exception of O(5), each oxygen in the iron hydroxide layer must be bonded to at least one cation in the layer in addition to those in the kyanite layer.

In addition, each oxygen in the iron hydroxide layer must have at least one cation vacancy adjacent to it.

Further examination of the structure determination of Smith (1968) allows for some tentative conclusions that reduce the large number of possible configurations allowed by Table 8. Smith found no sign of positional disorder except at the ivFe site. The absence of such displacements for Al(3A) suggests the probability that for each Al(3A) octahedron that is occupied, the adjacent P(1A) H positions (Fig. 3) are vacant. If the P(1A) sites were occupied, they most likely would be only partially occupied, causing small displacements of Al(3A) toward one side or the other of the octahedron dependent on the occupation of the two adjacent P(1A) sites. Thus the alternating occupancies of H and Al would prevent positional disorder of Al (Figs. 2, 3).

By contrast, Fe at the ivFe site does show positional (or temporal) disorder (Fig. 5). We suggest that the three subsidiary peaks around the ivFe site result from vacancy or occupancy of the P(1) sites. If two adjacent P(1) sites were empty, the Fe would be pulled slightly toward the O(1A)–O(1B) axis (Figs. 2, 3, 5). If one P(1) site were occupied and the adjacent one were empty, the Fe ions would be displaced slightly up or slightly down depending on whether the upper or lower P(1) site were vacant. If both adjacent sites were occupied, the Fe ion would be displaced away from the O(1A)–O(1B) axis. Figure 5 shows clearly that the alternate occupancy-vacancy situation for P(1) is most common, adjacent vacant sites are less common, and adjacent occupied sites do not occur when the tetrahedral Fe site is filled. For a
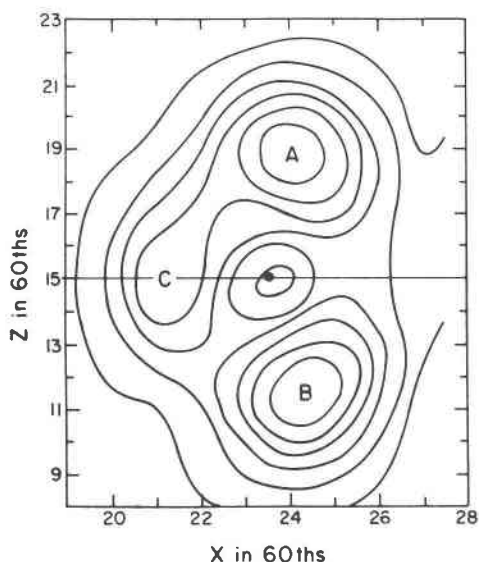
Fig. 5. Section through $(F_o - F_c)$ synthesis in the vicinity of the ^{iv}Fe site of staurolite. ^{iv}Fe site is marked by a dot, and A, B, and C are increased concentrations of electron density. The positions of P(1A) and P(1B) are to the left and at $z \geq 23/60$ and $\leq 9/60$. There is also an electron deficiency in the y direction above and below the ^{iv}Fe site indicating that most of the displacement of Fe is the x-z plane. After Smith (1968).

fully ordered staurolite without antiphase domains, this requires that *when the tetrahedral ^{iv}Fe site is filled*, Al occupies only Al(3A), H occupies only P(1B), and the 19% of vacancies that must exist in Al(3A) are *not* charge-balanced by occupied P(1A) sites.

The most common or "normal" configuration, that is, with the ^{iv}Fe, Al(3A), and P(1B) sites filled and the U sites vacant, is shown by "c" in Table 8. Note that each bond-valence sum designated by "c" is required by the "normal" configuration. Bond-valence sums to oxygens vary from 1.92 to 2.13 v.u. except for the few percent of cases where the bond-valence sum is reduced by 0.24 v.u. where ^{iv}Al replaces ^{iv}Si in the kyanite layer. This configuration could be used as the basis for an ideal formula, except for the fact that it is not in overall charge balance if eight Si are assumed. However, substitution of 6% ^{iv}Al for ^{iv}Si in the kyanite layer would provide overall charge balance, suggesting that Si-Al substitution is an intrinsic aspect of staurolite structure, which must be charge-balanced throughout. This is consistent with the maximum value of 7.8 Si ions pfu in the analyses of Table 4. In addition, all staurolites with tetrahedral sites filled have ≤ 4 H.

Whenever the ^{iv}Fe sites in staurolite are fully occupied, the H content is about 2.8 of the 4 P(1B) sites, or 70% occupied (Fig. 1). The 30% vacancy at the P(1B) site leads to an alternate "normal" configuration. In this configuration, designated "d" in Table 8, the ^{iv}Fe and Al(3A) sites are occupied whereas the P(1B) and U sites are vacant. Bond-valence sums range from 1.41 to 2.13 v.u. The 1.41 value to O(1B) must be increased by movement of Fe toward the O(1A)–O(1B) axis (Fig. 5). The P(1B) vacancies are charge-balanced by this movement of Fe and by the structure as a whole.

The third most common configuration, designated "e" in Table 8, occurs when Al(3A) sites are vacant. Charge-balance and bond-valence considerations suggest that in this configuration, P(1B) and U(1) should be occupied to provide a range of bond-valence

Table 9. Chemical substitutions in staurolite

Substitution	Sites	Charge-balance*	Range
Fe $\rightleftharpoons$ Mg $\rightleftharpoons$ Zn	^{iv}Fe	yes	extensive
Fe $\rightleftharpoons$ Mn	U(1)	yes	limited
Al $\rightleftharpoons$ Fe^{3+}	Al(3A)	yes	limited
Si $\rightleftharpoons$ Al	Si	no	limited
Fe + $\frac{1}{3}\square$ $\rightleftharpoons$ Li + $\frac{1}{3}$Al	^{iv}Fe, Al(3A)**	yes	extensive
Fe + $\frac{2}{3}$Al $\rightleftharpoons$ Ti + $\frac{2}{3}\square$	^{iv}Fe, Al(3A)†	yes	limited
Al + $\square$ $\rightleftharpoons$ $\square$ + Fe	Al(3A), U(1)	no	limited
Fe + 2$\square$ $\rightleftharpoons$ $\square$ + 2H	^{iv}Fe, P(1A,B)	yes	extensive

* In absence of charge balance, range is very limited and balance is achieved by remainder of structure.
** Dutrow et al., 1986.
† Substitution is speculative.

sums from 1.65 to 2.43 v.u. For the Pizzo Forno staurolite, the 12% U(1) occupancy satisfies some of the charge imbalance left by the 19% of the Al(3A) sites that are vacant. As with the previous two configurations, this substitution of a divalent ion at U(1) for a trivalent ion at Al(3A) does not lead to a *variable* substitution because the configuration is not charge-balanced. Occupancy of adjacent ^{iv}Fe and U sites produces a bond-valence sum of 2.43 v.u. on O(5). These values should be reduced somewhat by ^{iv}Fe positional disorder. In addition, such a configuration must occasionally occur at least in all staurolites for which the average U-site occupancy is more than the ^{iv}Fe deficiency. Thus we have a substitution module consisting of a few narrow strips through the structure, in which Al(3A) and P(1A) are empty and adjacent U(1) sites are filled (Figs. 2, 3). Continuity is suggested by the fact that each Al(3A) vacancy is partly compensated by U(1) occupancy on both sides, and vice versa.

Finally, we must consider the ^{iv}Fe-site vacancies in Pizzo Forno staurolite and the implications for variable composition in high-H, low-R^{2+} staurolites. The requirement of a vacant ^{iv}Fe site produces one of several possible configurations, as can be seen by inspection of Table 8. The possibilities are (1) Al(3A), P(1B) occupied; U(1), U(2) vacant; bond-valence sums 1.56–2.01 v.u.; (2) Al(3A), P(1B), and U(1) or U(2) occupied; bond-valence sums 1.56–2.01 v.u.; (3) Al(3A), P(1B), U(1), and U(2) occupied; bond-valence sums 1.93–2.19 v.u.; (4) P(1A) and P(1B) occupied; Al(3A), U(1), and U(2) vacant; bond-valence sums 1.59–1.99 v.u. The substitution produced by ^{iv}Fe vacancies almost certainly must involve an overall increase in H and a decrease in R^{2+} as shown by Figure 1. Thus, possibilities 2 and 3 are less probable because they involve increases in R^{2+} at the U sites. There is no substitution for case 1 that allows for charge balance. All the substitutions have some undesirable bond-valence sums. Only case 4 ("f" in Table 8) allows for a simple substitution module with two hydrogens in adjacent sites charge-balancing a neighboring R^{2+} at the ^{iv}Fe-site, according to R$^{2+}_{^{iv}Fe}$ + 2$\square$ $\rightleftharpoons$ $\square$ + 2H. Without this substitution, all staurolites (e.g., 77-55c) would contain ≤ 4 (H + F). The substitution allows H to increase to a value over 4, but limited by the occupancy of Al(3A). In staurolites with the highest H contents, the P(1A) and U(1) positions are filled adjacent to empty Al(3A) sites (configuration "g" in Table 8) leading to small changes in bond-valence. The substitution of two hydrogens for one R^{2+} occurs in all staurolites with ≥ 2.8 (H + F) and ≤ 4 tetrahedral (R^{2+} + Li + Ti).

Staurolite substitutions are listed in Table 9, beginning with those that do not change the configuration of the iron hydroxide layer and ending with those that do change the configuration of the layer. All substitutions may be thought of as proceeding from "normal" staurolite configuration

("c" and "d" in Table 8). Substitutions are broadly categorized as either limited or extensive. The most important substitutions are those that are variable, such as $R^{2+} + 2\square \rightleftharpoons \square + H$. The dashed line in Figure 1 is 0.4 ions pfu below the regression line and represents the estimated tetrahedral $(R^{2+} + Li + Ti)$. It is calculated by assuming 0.25 Fe^{3+} at the Al(3A) site, 0.25 (Fe + Mn) at the U(1) site, and 0.1 Ti at the tetrahedral site. Tetrahedral $(R^{2+} + Li + Ti)$ reaches a value of 4.06 at (H + F) = 2.8, suggesting that this is the lower limit of (H + F). If staurolites with lower values of (H + F) occur, then a substitution involving R^{2+} at U(2) sites might occur. Alternatively, a small amount of R^{2+} substitution might occur at Al(3A). An upper limit of 4.6 (H + F) is based on the assumption that the average number of Al(3A) vacancies may be fully occupied at P(1A) by two hydrogens each, in a maximum-H staurolite. Table 5 and Figure 1 show that the two Al(3A) sites are 85% occupied, assuming 0.25 Fe^{3+} ions at Al(3A). This leads to 4 (H + F) at P(1B) and 0.6 (H + F) at P(1A). Thus a reasonable range of substitution is from about 4 tetrahedral ions, 2.8 (H + F) to about 3.1 tetrahedral ions, 4.6 (H + F).

Although the chemistry, structure, and approximate bond-valence calculations support the substitutions listed in Table 9, staurolite is a very complex mineral whose crystal chemistry seems to be controlled more by local charge balance involving vacancies in the iron hydroxide layer than by formal substitutions. Thus these substitutions must be regarded as approximate mechanisms of providing charge balance. It is reasonable to expect that other substitutions not given here are responsible for some of the compositional variation and vacancy distribution. We believe we have identified the most important ones. Minor changes in the substitution schemes are needed to account for disorder.

Endmembers and approximate activity model

Because of the nonstoichiometric nature of staurolite, there exist no endmembers without solid solution. We propose that the best "endmembers" for staurolite are those that contain appropriate amounts of the solid solutions that occur in limited and roughty constant amounts in all staurolites. Calculations of the effects of these staurolite substitutions would be very difficult and would be highly dependent on chemical analyses at least as accurate as those presented here and preferably on structure determinations as well. We therefore choose realistic endmembers with either tetrahedral Fe sites filled or with maximum H. We propose the following with informal names:

$H_{2.8}Fe_4(Al_{17.46}Fe^{3+}_{0.25})Fe^{U(1)}_{0.25}(Si_{7.65}Al_{0.35})O_{48}$ Fe-dominant staurolite

Same with four tetrahedral Mg   Mg-dominant staurolite

Same with four tetrahedral Zn   Zn-dominant staurolite

$H_{4.6}Fe_{3.1}(Al_{17.46}Fe^{3+}_{0.25})Fe^{U(1)}_{0.25}(Si_{7.65}Al_{0.35})O_{48}$ H-dominant staurolite
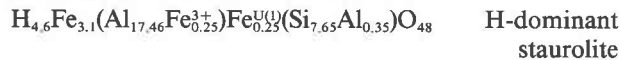
An *approximate* activity model for Fe-dominant staurolite is X^4_{ivFe}, where the mole fraction is of Fe at the

tetrahedral site, and vacancies are included as part of the remainder of the site. As the H-ion content is coupled to the vacancies at the ^{iv}Fe site, it need not be specified. In the absence of a structure determination, one must assume that Al(3A) and U(1) have 0.25 Fe^{3+} ions and 0.25 (Mn + Fe) ions, respectively, and that the remaining Fe is tetrahedral.

Stoichiometry from microprobe analyses

Because of the lack of information concerning both H and Li content, any estimate of stoichiometry from microprobe analyses can be very uncertain. This can be improved considerably with careful analyses for H and Li of a few representative staurolites from an area. In the absence of such analyses, the data of Tables 4 and 5 may be useful. One possibilty for estimating stoichiometry is discussed by Holdaway et al. (1986). For staurolites that coexist with garnet or biotite, average values are assumed for H and Li (3.06 and 0.2 ions pfu, respectively); for staurolites that do not coexist with biotite or garnet, 4.14 H ions are assumed. A second possibility, which should be useful for staurolites that formed under very reducing conditions with graphite and hematite-free ilmenite, is to assume (Al + Si) is 25.53. Agreement between the two methods implies that the stoichiometry is reasonable. Disagreement between the methods and low R^{2+} by the second method suggests the possibility of high Li. However, we stress that neither of these methods is of use in attempting to work out the crystal-chemical relations of a group of staurolites. Any procedure that involves estimating some quantity for staurolite will lead to imperfections in stoichiometric data.

Testing the crystal-chemical model

Although the present crystal-chemical model has significant supportive evidence, several aspects remain speculative. More staurolite structure determinations are needed to test and refine the proposed model. In addition, very careful and complete chemical analyses are needed. Efforts are under way by F. C. Hawthorne and by D. T. Griffen to determine additional structures of various staurolite compositions. The following questions should be examined specifically. (1) Is combined occupancy of U sites approximately constant? (2) Is ^{iv}Fe-site positional disorder present in all staurolites, and is there positional disorder for other ions, e.g., at Al(3A)? (3) Do the Al(3A) + Al(3B) occupancies vary between staurolites? (4) In what site is Li in high-Li staurolite? (5) Can most of the Mg of Mg-rich staurolites be assigned to the ^{iv}Fe site? Problems continue to exist concerning the importance and location of Fe^{3+} and the location of Ti and Mn.

PETROLOGIC CONSIDERATIONS

Most petrologic treatments of staurolite have suffered from an oversimplified concept of the nature of the mineral. The problems in correlating staurolite stability data with temperatures indicated by other methods result at least as much from these oversimplifications as from in-
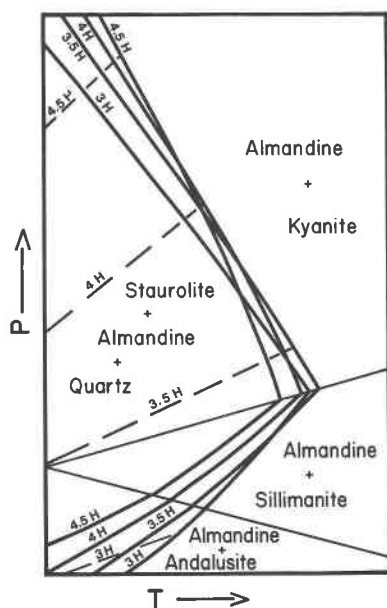
Fig. 6.   Schematic $P\text{-}T$ plot to show (1) how staurolite H content varies as a function of P and T when staurolite coexists with pure H_2O, almandine, and quartz (dashed lines) and (2) staurolite dehydration curves for various fixed amounts of H in staurolite (solid lines). An envelope around these dehydration curves defines the stable staurolite breakdown curve. H content of staurolite with its reaction products must vary smoothly as T increases and/or P decreases.

accurate stability data. We will attempt to clarify a few of these problems.

Effect of R^{2+} ionic radii

The sizes of the Al(3A), ^{iv}Fe, and U sites in staurolite appear to be very restricted. Mean size of the ^{iv}Fe for the present staurolites is inferred to vary between 0.616 and 0.637 (Fig. 4). These values, somewhat below the effective ionic radius of Fe^{2+} in staurolite ^{iv}Fe sites (0.655), may decrease for staurolites that formed at high pressure, where the structure is compressed. If the various Si and Al sites in the structure remain approximately the same in composition at high pressures, the effect of pressure on the ^{iv}Fe site would be to reduce its size and make it more favorable for the smaller constituents such as Mg, Li, Zn, and vacancies. At a given pressure, the radii suggest that the saturation limit would be Li $\geq$ Mg $\simeq$ Zn $\geq$ tetrahedral vacancies. As pressure increases, one may expect the saturation limits to increase. One may also expect to find that staurolites that formed at normal P, but were enriched in one of the small ions Li, Mg, or Zn will tend to be low in the others so that the mean ^{iv}Fe-site radius is relatively increased by larger amounts of Fe. Staurolites very high in Fe, to the exclusion of most other (R^{2+} + Li), are probably low-P staurolites.

Nature of experimental equilibria

The composition of staurolite in any experimental or natural system depends significantly on $f_{(H_2O)}$ and $a_{(FeO)}$, as

seen by the reaction

$$H_{4.6}Fe_{3.6}Al_{17.81}Si_{7.65}O_{48} + 0.36Fe_3Al_2Si_3O_{12}$$
$$\text{in staurolite} \qquad \text{in garnet}$$

$$= 1.04H_{2.8}Fe_{4.5}Al_{17.81}Si_{7.65}O_{48} + 0.774SiO_2 + 0.844H_2O.$$
$$\text{in staurolite}$$
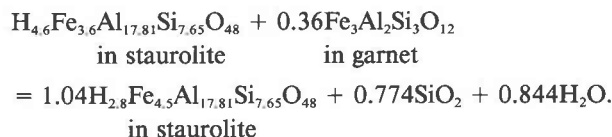
Lines of constant staurolite hydration state may be expected to have positive $P_{H_2O}\text{-}T$ slope, and it should be possible to contour the composition of staurolite with almandine and quartz in a fashion somewhat analogous to contouring the H_2O content of cordierite (Helgeson et al., 1978). In the absence of an R^{2+} phase such as almandine or biotite, the equilibrium favors more H-rich staurolite. Thus it is reasonable to expect that, at high-P and low-T conditions where staurolite first forms from chloritoid, the H content should be over 4, especially if garnet or biotite is absent. At higher temperatures, as staurolite breaks down to garnet and kyanite, H content should decrease. The lowest H content in a pure H_2O system, perhaps near 3, would be expected where staurolite breaks down at lower P to sillimanite or andalusite with garnet.

Efforts to retrieve thermodynamic data, extrapolate experimental equilibria, and decide between two and four hydrogens for staurolite (Yardley, 1981; Pigage and Greenwood, 1982; Anovitz and Essene, 1982) have not been very successful at low P and have indicated that the experimental data of Richardson (1968) are at temperatures that are too high. These results are partly due to the assumption of constant H in staurolite, which is probably reasonably accurate for the breakdown of chloritoid to staurolite in the high-P, low-T parts of the kyanite field, but which becomes increasingly inaccurate at higher T and lower P. The metastable curve for four-hydrogen staurolites in the sillimanite field will fall at lower temperatures than the stable three-hydrogen curve, as illustrated in Figure 6. If all experimental staurolite equilibria are to be related to a single staurolite composition (Fe-dominant staurolite), activity adjustments will be needed for staurolite breakdown compositions such that most experimental staurolites will have activities below one. Alternatively, the reaction must be changed for various positions along the curve.

Figure 6 is a schematic $P\text{-}T$ diagram illustrating these relationships. In the presence of pure H_2O, the stable composition of staurolite with almandine is determined by the family of staurolite-almandine curves. Metastable staurolite breakdown curves for hydrous states above or below the stable composition lie within the staurolite stability field. The envelope around these metastable curves is the stable staurolite breakdown curve, and it must vary smoothly in composition as T increases and/or P decreases. Because the staurolite-almandine curves may be subparallel to the breakdown curve in the sillimanite field, the hydration state of staurolite in pure H_2O may not change much along the breakdown reaction in the sillimanite field. Dilution of the fluid phase by CO_2 or CH_4 from reaction of H_2O with graphite will decrease the H

content of staurolite, and absence of an FeO-saturating phase will increase it.

Application to natural occurrences

Before relating variable H content of staurolite to natural occurrences, it is important to consider the effect of variations in $a_{Al_2O_3}$ vs. a_{SiO_2} on staurolite, as there is a slight Al-Si variability in staurolite compositions. In order to do this, we have placed the 28 staurolites that can be assumed to be reasonably low in Fe^{3+} in two groups: (1) occurrence with quartz and (2) occurrence with quartz and an Al_2SiO_5 phase. Nineteen staurolites with quartz have Al/Si = 2.327 ± 0.035, and nine staurolites with quartz and Al_2SiO_5 have Al/Si = 2.334 ± 0.037, suggesting that other factors such as Fe^{3+}, Li, and Ti are more important than relative activities of Al_2O_3 and SiO_2 in determining the Al/Si ratio.

In order to get some idea of the effect of P-T-X_{H_2O} and mineral assemblage on the H content of natural staurolites, we grouped the analyzed staurolites (Tables 1, 4) according to presence or absence of graphite, presence or absence of biotite or almandine, and nature of the Al_2SiO_5 phase when it coexisted with staurolite and biotite or garnet. In graphite-bearing assemblages, staurolite has H contents from 2.71 to 3.27 pfu, whereas in graphite-absent assemblages, H contents in staurolite ranges from 2.70 to 4.19. Those staurolites that coexist with biotite or garnet have H contents from 2.68 to 3.41 pfu, whereas those that do not coexist with biotite or garnet include two incomplete assemblages (H = 3.03 and 3.10), and three staurolites with H between 4.09 and 4.16. For all staurolites that coexist with a breakdown assemblage of Al_2SiO_5 and biotite or garnet, one staurolite with andalusite has H = 2.68 pfu, four with sillimanite have H = 2.85–3.29, and five with kyanite have H = 2.97–3.41. It seems that all these factors are affecting the H content of staurolite by controlling f_{H_2O} and a_{FeO}. Additional studies involving H analyses would be very useful to explain the controls in more detail at various P-T conditions, fluid compositions, and FeO activities. Staurolite has an advantage over cordierite as a fluid monitor because it presumably retains the H content of crystallization.

CONCLUSIONS

1. Complete and accurate staurolite analyses show that (Al + Si) and (R^{2+} + Li + ½H) behave as two nearly fixed element groups and suggest that the major substitutions are Si ⇌ Al, Fe ⇌ Mg ⇌ Zn ⇌ Li ⇌ Mn, 2H ⇌ (R^{2+} + Li).

2. The analyses provide evidence that Smith's (1968) structure analysis should be modified so that Si and Al are mainly the kyanite layer, Al (and Fe^{3+}?) are mainly at the Al(3A) sites, and (R^{2+} + Li) are mainly at the ^{iv}Fe and U(1) sites. The pseudo-orthorhombic symmetry and existence of antiphase domains in some staurolites, combined with the absence of positional disorder at Al(3) suggest that in fully ordered staurolite, the Al(3) octahedra

alternate between Al(3A) occupied by Al and P(1B) occupied by H.

3. Mean tetrahedral radius data can only be made consistent for various staurolites by using a small size for ^{iv}Fe-site vacancies (≤0.57 Å). Oxygen–cation distances for the ^{iv}Fe site require that to be applied to the ^{iv}Fe site, average Shannon (1976) ionic radii should be increased by 0.025 Å, consistent with positional (or temporal) disorder at the site. Present results provide support for the Griffen (1981) radius for tetrahedral Zn in staurolite.

4. Consideration of bond-valence calculations, the modified structure model, disorder at the ^{iv}Fe site, and the compositional variation of staurolites leads to a group of specific substitutions: (1) ^{iv}Si ⇌ ^{iv}Al is charge-balanced over the structure; (2) Al + □ ⇌ □ + R^{2+} compensates for a very narrow substitution range at Al(3A) with ions at U(1) producing partial charge balance; (3) R^{2+} + 2□ ⇌ □ + 2H compensates for tetrahedral Fe vacancies by occupation of adjacent P(1B) and P(1A) sites. This substitution is responsible for the variation at H and R^{2+} that occurs in staurolite.

5. The best endmembers for staurolite are those with tetrahedral sites filled and those with maximum H. An approximate activity model for Fe-dominant staurolite is X^4_{ivFe}. Relative differences in H and total R^{2+} must be accounted for in application of staurolite stability data. For determination of stoichiometries, a normalization scheme that fixes H and Li—or one that for staurolites that grew under reducing conditions sets (Al + Si) = 25.53—is suggested. However, this approach will not allow very meaningful estimates of H and Li unless representative H and Li analyses are completed.

6. Most sites in staurolite have very restricted ranges of occupancies and thus cannot vary much in size. The one metal-ion site that can have significant variation in occupancy, the ^{iv}Fe site, may favor smaller ions at higher pressures. At a given P and T, the saturation limit of Li is expected to be ≥ Mg ≃ Zn ≥ tetrahedral vacancies in the site.

REFERENCES

Albee, A.L., and Ray, L. (1970) Correction factors for electron probe microanalysis of silicates, oxides, carbonates, phosphates and sulfates. Analytical Chemistry, 42, 1408–1414.

Anovitz, L.M., and Essene, E.J. (1982) Phase equilibria in the

system Fe-Al-Si-O-H. Geological Society of America Abstracts with Programs, 14, 434.

Bancroft, G.M., Maddock, A.G., and Burns, R.G. (1967) Applications of the Mössbauer effect to silicate mineralogy—I. Iron silicates of known crystal structure. Geochimica et Cosmochimica Acta, 31, 2219–2246.

Bence, A.E., and Albee, A.L. (1968) Empirical correction factors for electron microanalysis of silicates and oxides. Journal of Geology, 76, 382–403.

Bence, A.E., and Holzwarth, W. (1977) Non-linearities of electron microprobe matrix corrections in the system MgO-Al$_2$O$_3$-SiO$_2$. 8th International Conference on X-ray Optics and Microanalysis 38A–38D.

Borg, I.Y., and Smith, D.K. (1969) Calculated X-ray powder patterns for silicate minerals. Geological Society of America Memoir 122.

Brown, I.D. (1981) The bond-valence method: An empirical approach to chemical structure and bonding. In M. O'Keefe and A. Navrotsky, Eds. Structure and bonding in crystals, volume 2, 1–30. Academic Press, New York.

Deer, W.A., Howie, R.A., and Zussman, J. (1962) Rock-forming minerals, volume 1, Ortho- and Ring Silicates. Wiley, New York.

Dickson, B.L., and Smith, G. (1976) Low-temperatue optical absorption and Mössbauer spectra of staurolite and spinel. Canadian Mineralogist, 14, 206–215.

Donnay, J.D.H., and Donnay, G. (1983) The staurolite story. Tschermaks Mineralogische und Petrographische Mitteilungen, 31, 1–15.

Dowty, Eric. (1972) Site distribution of iron in staurolite. Earth and Planetary Science Letters, 15, 72–74.

Dutrow, B.L., Holdaway, M.J., and Hinton, R.W. (1986) Lithium in staurolite: Its petrologic significance. Contributions to Mineralogy and Petrology, in press.

Evans, H.T., Jr., Appleman, D.E., and Handwerker, D.S. (1963) The least squares refinement of crystal unit cells with powder diffraction data by an automatic computer indexing method. (abs.) American Crystallographers Association Annual Meeting, Cambridge, Massachusetts, Program, 42–43.

Fitzpatrick, J.J. (1976) Studies in the microstructure and crystal chemistry of minerals. Ph.D. thesis, University of California, Berkeley.

Fritz, S.F., and Popp, R.K. (1985) A single-dissolution technique for determining FeO and Fe$_2$O$_3$ in rock and mineral samples. American Mineralogist, 70, 961–968.

Froese, Edgar, and Gasparrini, Elvira. (1975) Metamorphic zones in the Snow Lake area, Manitoba. Canadian Mineralogist, 13, 162–167.

Ganguly, Jibamitra. (1972) Staurolite stability and related parageneses: Theory, experiments, and applications. Journal of Petrology, 13, 335–365.

Ganguly, Jibamitra, and Saxena, S.K. (1984) Mixing properties of aluminosilicate garnets: Constraints from natural and experimental data, and applications to geothermo-barometry. American Mineralogist, 69, 88–97.

Green, J. C. (1963) High-level metamorphism of pelitic rocks in northern New Hampshire. American Mineralogist, 48, 991–1023.

Griffen, D.T. (1981) Synthetic Fe/Zn staurolites and the ionic radius of ^{iv}Zn^{2+}. American Mineralogist, 66, 932–937.

Griffen, D.T., and Ribbe, P. H. (1973) The crystal chemistry of staurolite. American Journal of Science, 273-A, 479–495.

Griffen, D.T., Gosney, T.C., and Phillips, W.R. (1982) The chemical formula of natural staurolite. American Mineralogist, 67, 292–297.

Guidotti, C.V. (1974) Transition from staurolite to sillimanite zone, Rangely quadrangle, Maine. Geological Society of America Bulletin, 85, 475–490.

Hanisch, K. (1966) Zur Kenntris der Kristallstrucktur von Staurolith. Neues Jahrbuch für Mineralogie Monatshefte, 362–366.

Helgeson, H.C., Delany, J.M., Nesbitt, H.W., and Bird, D.K.

(1978) Summary and critique of the thermodynamic properties of rock-forming minerals. American Journal of Science, 278-A, 1–229.

Hemingway, B.S., and Robie, R.A. (1984) Heat capacity and thermodynamic functions for gehlenite and staurolite: With comments on the Schottky anomaly in the heat capacity of staurolite. American Mineralogist, 69, 307–318.

Holdaway, M.J., Dutrow, B.L., Borthwick, James, Shore, Patrick, Harmon, R.S., and Hinton, R.W. (1986) H content of staurolite as determined by H extraction line and ion microprobe. American Mineralogist, 71, 1135–1141.

Hounslow, A.W., and Moore, J.M. (1967) Chemical petrology of Grenville schists near Fernleigh, Ontario. Journal of Petrology, 8, 1–28.

Juurinen, Aarno. (1956) Composition and properties of staurolite. Annales Academiae Scientiarum Fennicae, Series A, III Geology, 47, 1–53.

Kretz, Ralph. (1983) Symbols for rock-forming minerals. American Mineralogist, 68, 277–279.

Lonker, S.W. (1983) The hydroxyl content of staurolite. Contributions to Mineralogy and Petrology, 84, 36–42.

Nárary-Szabó, I., and Sasvári, K. (1958) On the structure of staurolite HFe$_2$Al$_9$Si$_4$O$_{24}$. Acta Crystallographica, 11, 862–865.

Novak, J.M., and Holdaway, M.J. (1981) Metamorphic petrology, mineral equilibria, and polymetamorphism in the Augusta quadrangle, south-central Maine. American Mineralogist, 66, 51–69.

Ohmoto, Hiroshi, and Kerrick, D.M. (1977) Devolatilization equilibria in graphitic systems. American Journal of Science, 277, 1013–1044.

Osberg, P.H. (1971) An equilibrium model for buchan-type metamorphic rocks, south-central Maine. American Mineralogist, 56, 570–586.

Pigage, L.C., and Greenwood, H.J. (1982) Internally consistent estimates of pressure and temperature: The staurolite problem. American Journal of Science, 282, 943–969.

Rao, B.B., and Johannes, W. (1979) Further data on the stability of staurolite + quartz and related assemblages. Neues Jahrbuch für Mineralogie Monatshefte, 437–447.

Regnard, J.R. (1976) Mössbauer study of natural crystals of staurolite. Journal de Physique, 37, C6-797–800.

Ribbe, P.H. (1982) Staurolite. In P.H. Ribbe, Ed. Orthosilicates, reviews in mineralogy, volume 5, 171–187. Mineralogical Society of America, Washington, D.C.

Richardson, S.W. (1968) Staurolite stability in a part of the system Fe-Al-Si-O-H. Journal of Petrology, 9, 467–488.

Rumble, Douglas, III. (1978) Mineralogy, petrology, and oxygen isotopic geochemistry of the Clough Formation, Black Mountain, western New Hampshire, U.S.A. Journal of Petrology, 19, 317–340.

Schreyer, W., and Seifert, F. (1969) High-pressure phases in the system MgO-Al$_2$O$_3$-SiO$_2$-H$_2$O. American Journal of Science, 267-A, 407–443.

Schreyer, W., Horrocks, P.C., and Abraham, K. (1984) High-magnesium staurolite in a sapphirine-garnet rock from the Limpopo Belt, Southern Africa. Contributions to Mineralogy and Petrology, 86, 200–207.

Scorzelli, R.B., Baggio-Saitovitch, E., and Danon, J. (1976) Mössbauer spectra and electron exchange in tourmaline and staurolite. Journal de Physique, 37, C6-801–805.

Shannon, R.D. (1976) Revised effective ionic radii and systematic studies of interatomic distances in halides and chalcogenides. Acta Crystallographica, A32, 751–767.

Smith, J.V. (1968) The crystal structure of staurolite. American Mineralogist, 53, 1139–1155.

Spear, F.S. (1982) Phase equilibria of amphibolites from the Post Pond Volcanics, Mt. Cube quadrangle, Vermont. Journal of Petrology, 23, 383–426.

Tagai, T., and Joswig, W. (1985) Untersuchungen der Kationenverteilung im Staurolith durch Neutronenbeugung bei 100 K. Neues Jahrbuch für Mineralogie Monatshefte, 97–107.

Takéuchi, Y., Aikawa, N., and Yamamoto, T. (1972) The hydrogen locations and chemical composition of staurolite. Zeitschrift für Kristallographie, 136, 1–22.

Taylor, F.C., and Schiller, E.A. (1966) Metamorphism of the Meguma Group of Nova Scotia. Canadian Journal of Earth Sciences, 3, 959–974.

Ward, C.M. (1984a) Magnesium staurolite and green chromian staurolite from Fiordland, New Zealand. American Mineralogist, 69, 531–540.

——— (1984b) Titanium and the color of staurolite. American Mineralogist, 69, 541–545.

Wenk, H.-R., Wenk, E., and Wallace, J.H. (1974) Metamorophic mineral assemblages in pelitic rocks of the Bergell Alps. Schweizerische Mineralogische und Petrographische Mitteilungen, 54, 507–554.

Winter, J.K., and Ghose, Subrata. (1979) Thermal expansion and high-temperature crystal chemistry of the Al_2SiO_5 polymorphs. American Mineralogist, 64, 573–586.

Yardley, B.W.D. (1981) A note on the composition and stability of Fe-staurolite. Neues Jahrbuch für Mineralogie Monatshefte, 127–132.

York, D. (1966) Least-squares fitting of a straight line. Canadian Journal of Physics, 44, 1079–1086.

Zen, E-an. (1981) Metamorphic mineral assemblages of slightly calcic pelitic rocks in and around the Taconic allochthon, southwestern Massachusetts and adjacent Connecticut and New York. U.S. Geological Survey Professional Paper 1113.